1-1-1966

Hypersonic Flow of Dissociating Air Past a Circular Cone UARI Research Report No. 26

Jurgen Thoenes

UARI Research Report No. 26

Master

HYPERSONIC FLOW OF DISSOCIATING AIR PAST A CIRCULAR CONE

by

Jurgen Thoenes

Final Technical Report

This work was supported by
the U. S. Army Missile Command under
Contract No. DA-01-021-AMC-12039 (Z)

University of Alabama Research Institute
Huntsville, Alabama
January 1966

UARI Research Report No. 26

HYPERSONIC FLOW OF DISSOCIATING AIR PAST A CIRCULAR CONE

by

Jurgen Thoenes

Final Technical Report

This work was supported by
the U. S. Army Missile Command under
Contract No. DA-01-021-AMC-12039 (Z)

University of Alabama Research Institute
Huntsville, Alabama
January 1966

FOREWORD

The research reported herein was sponsored by the U. S. Army Missile Command under Contract No. DA-01-021-AMC-12039(Z). This work has been conducted as a continuation of Contract No. DA-01-009-AMC-166(Z), entitled "Basic Research in the Field of Inviscid High Temperature Hypersonic Flow of Air Past Pointed Bodies of Revolution." The Technical Monitor of this contract was Dr. Bernard J. Steverding.

The author is indebted to Dr. Rudolf Hermann, Director of the University of Alabama Research Institute, for directing the work on this contract, and for rendering valuable criticism during the preparation of this report. The efforts of Mr. K. V. Ramakrishna in checking the equations are gratefully acknowledged.

Last but not least, the author feels obliged to Mr. Robert A. McGraw for programming the equations for equilibrium flow, and to Mr. Ronald J. Fischer for programming the problem of nonequilibrium flow.

ABSTRACT

This report discusses two methods for the calculation of hypersonic flow of dissociating air past a circular cone. One objective of the investigation was to apply a Taylor-Maccoll type analysis in order to calculate chemical equilibrium flow past a circular cone and to compare the results with those previously obtained from Dorodnitsyn's integral method. The other objective was to investigate improvements to the one-strip integral method by developing and using a two-strip analysis for the calculation of chemical nonequilibrium cone flow. It was found that, for equilibrium flow, the results from the Taylor-Maccoll type analysis are in excellent agreement with those from the one-strip integral method. For nonequilibrium flow, it is shown that with increasing distance away from the tip the two-strip solution is closer to the equilibrium flow solution than the standard one-strip solution is. It is interesting to notice that, except for the distribution of the shock wave angle and the cone surface velocity, at a sufficient distance from the tip, the one-strip semi-exact solution approaches the equilibrium flow solution still closer than the two-strip solution does.

TABLE OF CONTENTS

LIST OF FIGURES

APPENDICES

NOMENCLATURE

A	Expression, defined by eq. (4.63)
A_i	Expressions, defined in Appendix C
a	Expression, defined by eq. (D-58)
a_{ij}	Coefficients, defined in Appendix C
B	Expression, defined by eq. (4.64)
B_i	Expressions, defined in Appendix D
b	Constant, defined by eq. (2.6)
b_{ij}	Coefficients, defined in Appendix D
C	Number of oxygen atoms per unit mass of gas
C_i	Expressions, defined in Appendix B and C
D'_{02}	Characteristic temperature of oxygen dissociation [^{o}K]
$\vec{e}_i$	Unit vectors
F_i	Expressions, defined by eq. (3.16) through (3.18)
f	Source function, defined by eq. (2.9)
h	Enthalpy [J/kg]
h_t	Total enthalpy [J/kg]
K_c	Concentration equilibrium constant [particles/m^3]
K_p	Pressure equilibrium constant [N/m^2]
k_d	Dissociation rate constant [m^3/particle · sec]
L	Expression, defined on p. 19
l	Characteristic length [m], defined on p. 28
M_1	Free stream Mach number
n_i	Number density of ith species
p	Pressure [N/m^2]
$\vec{q}$	Velocity vector
q	Resultant velocity [m/sec]
R	Gas constant of undissociated gas [J/kg ^{o}K]
r	Radial coordinate (for equilibrium flow see Fig. 1, for nonequilibrium flow see Fig. 9)

S	Expression, defined on p. 19
T	Temperature $[{}^{o}K]$
u, v, w	Velocity components for equilibrium flow in r, θ, ϕ direction, respectively
u, v	Velocity components for nonequilibrium flow in x, y direction, respectively
x, y	Coordinates, see Fig. 9
Z	Compressibility factor
α	Degree of oxygen dissociation
β	Angle, defined in Fig. 9
δ	Dimensionless shock coordinate, defined by eq. (4.26)
ξ, η	Dimensionless x, y coordinate, respectively
ρ	Mass density $[kg/m^3]$
θ, θ_b	Angular coordinate or cone semi-vertex angle
θ_{O2}	Characteristic vibrational temperature of oxygen, $[{}^{o}K]$
θ_{N2}	Characteristic vibrational temperature of nitrogen, $[{}^{o}K]$
σ	Shock wave angle
ϕ	Circumferential coordinate

Subscripts

1	Free stream
b	Body surface
2	Strip interface
s	Behind shock wave
O2	Oxygen
N2	Nitrogen

SECTION I
INTRODUCTION

The problem considered in the present paper is that of inviscid high enthalpy, chemically reacting flow of air past a circular cone at hypersonic velocities. Also investigated is the effect of free stream oxygen dissociation on the various flow field parameters. This work should be considered as a continuation and as an extension of previous work (Ref. 1) which treated chemically frozen, equilibrium, and nonequilibrium conical flows, using Dorodnitsyn's method of integral relations in its one-strip version, also called the first approximation.

The present report deals with two cases which may be considered rather independent of each other. As done previously, the investigation is based on a simplified air model, in which air is approximated by a three-component gas (O_2, O, N_2), valid in the range of oxygen dissociation.

First, inviscid conical flow of air in chemical and vibrational equilibrium is calculated by using a Taylor-Maccoll type analysis. The purpose of these calculations is to compare the accuracy of the previously used integral method with that of a well established, so to speak, classical method. In section III the equations for supersonic conical flows as first derived by Taylor and Maccoll (Ref. 2) are combined with the necessary thermodynamic equations. While Taylor and Maccoll treated their perfect gas calculations as a direct problem, which means that the flow field is calculated for a specified cone angle, an inverse approach was used in the present investigation. In this way the shock wave angle is specified, and the associated cone vertex angle is determined from the calculation. This procedure avoids any iterative schemes which would be necessary in the direct approach.

Secondly, in section IV chemical nonequilibrium flow of air past a circular cone is treated by using Dorodnitsyn's integral method in its two-strip version, also called the second approximation. To the author's knowledge, neither the one-strip nor the two-strip integral method has ever been applied by other authors to the calculation of chemically relaxing flow of air past cones, although a similar case of vibrational relaxation in a pure diatomic gas has been treated by South (Ref. 3). Results from the present calculations can, therefore, be compared only with the author's previous calculations (Ref. 1).

SECTION II

FORMULATION OF THE PROBLEM

2.1 Basic Equations

This section presents the basic equations for the two cases which are mentioned in the introduction and which will subsequently be discussed in detail. For the derivation of all equations stated in this section, the reader is referred to Ref. 1.

Neglecting viscosity, the basic equations for steady, adiabatic flow are the following:

Conservation of mass:

$$\nabla \cdot (\rho \vec{q}) = 0 \tag{2.1}$$

Conservation of momentum:

$$\nabla \left(\frac{q^2}{2} \right) + (\nabla \times \vec{q}) \times \vec{q} + \frac{1}{\rho} \nabla p = 0 \tag{2.2}$$

Conservation of energy:

$$h + \frac{q^2}{2} = h_t = \text{const} \tag{2.3}$$

The above equations are the usual equations of motion, and they do not depend on any particular gas model. In order to solve a given problem, they must be supplemented by expressions describing the relation of the thermodynamic variables among each other. These expressions always depend on the particular gas model used.

The simplified air model used in this investigation consists of a three component reacting gas (O_2, O, N_2), a detailed description of which can be found in Ref. 1.

Defining the degree of oxygen dissociation, α, as the ratio of the mass of oxygen in dissociated form to the total mass of oxygen in the mixture, the following equations can be obtained:

$$p = \rho RZT \tag{2.4}$$

where

$$Z = 1 + b\alpha \tag{2.5}$$

and

$$b = \frac{n_{O2}}{n_{O2} + n_{N2}} = 0.21 \tag{2.6}$$

Considering translational, rotational, and vibrational motion of the particles in the mixture, the enthalpy may be written as

$$h = R\left[b\alpha D'_{O2} + \frac{3}{2}b\alpha T + \frac{7}{2}T + \frac{(1-\alpha)b\theta_{O2}}{e^{\theta_{O2}/T} - 1} + \frac{(1-b)\theta_{N2}}{e^{\theta_{N2}/T} - 1}\right] \tag{2.7}$$

In the case of chemical nonequilibrium flow, the composition of the gas is controlled by the reaction rates of the chemical processes which are included. In the present calculations, only oxygen dissociation is considered; and the resulting rate equation can be written as

$$\vec{q} \cdot \nabla \alpha = f \tag{2.8}$$

where f is the source function given by

$$f = \frac{C^2 \rho^2 Z k_d}{2b}\left[\frac{1-\alpha}{2C\rho} - \frac{\alpha^2}{K_c}\right] \tag{2.9}$$

Expressions for the dissociation rate constant k_d, and the concentration equilibrium constant K_c are given in Appendix A.

If it is assumed that the air is in instantaneous equilibrium between the shock wave and the body, the pressure, temperature, and degree of dissociation are always related by the equilibrium relation

$$\frac{K_p(T)}{p} = \frac{4b\alpha^2}{(1-\alpha)Z} \tag{2.10}$$

where $K_p(T)$ is the pressure equilibrium constant, which is a function of temperature, and which is also given in Appendix A.

2.2 Boundary Conditions

The flow in the shock layer is bounded by the shock wave on one side and by the body surface on the other side. For explicit calculations, the conditions at these boundaries must be specified.

In all cases the condition for flow tangency at the body surface is given by

$$v = 0 \tag{2.11}$$

As far as the conditions on the downstream side of the shock wave are concerned, these can be obtained from the principles of conservation of mass, momentum, and energy across the shock wave. For equilibrium flow, the gas is assumed to be in thermodynamic equilibrium behind the shock; for nonequilibrium flow, the frozen state is assumed behind the shock. Detailed equations for both cases may be found in Ref. 1 and are, therefore, not repeated here.

SECTION III

EQUILIBRIUM FLOW PAST A CIRCULAR CONE

3.1 Basic Assumptions

As early as 1929, A. Busemann (Ref. 4) has stated that supersonic inviscid conical flows are characterized by the fact that in the shock layer the pressure and the velocity vector are constant on coaxial conical surfaces having the same vertex as the conical body. Assuming this behavior of the flow, in which all variables such as pressure, density, and velocity are functions of θ (see Fig. 1) only, Taylor and Maccoll (Ref. 2) successfully calculated supersonic conical flow of a perfect gas in 1933. The same assumptions will be the basis of the present calculations.

3.2 Conical Flow Equations

For axisymmetric flows, the governing equations are most suitably expressed in pherical coordinates (Fig. 2). Since the flow variables are independent of the circumferential coordinate ϕ, only two independent variables, namely r and θ, are retained. Finally the assumption that all flow variables are constant along any radius vector through the apex of the cone reduces the independent variables to θ alone.

Hence, with

$$\nabla p = \frac{\partial p}{\partial r}\,\vec{e}_r + \frac{1}{r}\,\frac{\partial p}{\partial \theta}\vec{e}_\theta + \frac{1}{r \sin\theta}\,\frac{\partial p}{\partial \phi}\,\vec{e}_\phi \tag{3.1}$$

$$\nabla \cdot \vec{q} = \frac{1}{r^2}\,\frac{\partial}{\partial r}(r^2 u) + \frac{1}{r\sin\theta}\,\frac{\partial}{\partial\theta}(v \sin\theta) + \frac{1}{r\sin\theta}\,\frac{\partial w}{\partial \phi} \tag{3.2}$$

and

$$\nabla \times \vec{q} = \frac{1}{r\sin\theta}\left[\frac{\partial}{\partial\theta}(w\sin\theta) - \frac{\partial v}{\partial\phi}\right]\vec{e}_r + \frac{1}{r}\left[\frac{1}{\sin\theta}\,\frac{\partial u}{\partial\phi} - \frac{\partial}{\partial r}(rw)\right]\vec{e}_\theta + \frac{1}{r}\left[\frac{\partial}{\partial r}(rv) - \frac{\partial u}{\partial\theta}\right]\vec{e}_\phi \tag{3.3}$$

the following equations are obtained from eq. (2.1) and (2.2):

Conservation of mass:

$$\frac{dv}{d\theta} + v\left(\frac{1}{\rho}\frac{d\rho}{d\theta} + \cot\theta\right) + 2u = 0 \tag{3.4}$$

r-Momentum:

$$\frac{du}{d\theta} - v = 0 \tag{3.5}$$

θ-Momentum:

$$v\left(u + \frac{dv}{d\theta}\right) + \frac{1}{\rho}\frac{dp}{d\theta} = 0 \tag{3.6}$$

It should be noticed that in this particular application the r-momentum equation reduces to the irrotationality condition

$$\nabla \times \vec{q} = 0 \tag{3.7}$$

Therefore, it follows that in the flow under consideration the assumption of homenergic and irrotational (hence, also homentropic) flow upstream of the shock wave, together with the assumption of instantaneous equilibrium downstream of the shock wave, means that the flow in the shock layer is also homenergic and irrotational (and thus homentropic).

Eq. (2.3), (2.4), (2.10), and (3.4) through (3.6) now form a system of six equations for the six unknowns: u, v, p, ρ, T, and α. The derivative of v, obtained from the θ-momentum equation, can be substituted into the continuity equation and the differentiated energy equation. Also differentiating the equation of state and the equilibrium relation, the resulting system of equations for the derivatives of p, ρ, T, and α is as follows:

Continuity:

$$\frac{1}{\rho v}\frac{dp}{d\theta} - v\left(\frac{1}{\rho}\frac{d\rho}{d\theta} + \cot\theta\right) - u = 0 \tag{3.8}$$

Energy:

$$\frac{1}{\rho}\frac{dp}{d\theta} - \left(\frac{\partial h}{\partial T}\right)_{\alpha}\frac{dT}{d\theta} - \left(\frac{\partial h}{\partial T}\right)_{\alpha}\frac{d\alpha}{d\theta} = 0 \tag{3.9}$$

State:

$$\frac{dp}{d\theta} - RZT\frac{d\rho}{d\theta} - \rho RZ\frac{dT}{d\theta} - \rho RTb\frac{d\alpha}{d\theta} = 0 \qquad (3.10)$$

Equilibrium Relation:

$$4b\alpha^2\frac{dp}{d\theta} - (1-\alpha)\,Z\left(\frac{dK_p}{dT}\right)\frac{dT}{d\theta} + \frac{4b\alpha p\,[Z+(1-\alpha)]}{(1-\alpha)Z}\frac{d\alpha}{d\theta} = 0 \qquad (3.11)$$

Eliminating the derivative of p from the above equations and solving for the remaining derivatives, the following expressions are finally obtained:

$$\frac{dp}{d\theta} = \frac{\rho v\,F_3(v\cot\theta + u)}{p - v^2F_3} \qquad (3.12)$$

$$\frac{d\alpha}{d\theta} = v(v\cot\theta + u)\,\frac{F_1}{F_2}\left(1 + \frac{v^2F_3}{p - v^2F_3}\right) \qquad (3.13)$$

$$\frac{dT}{d\theta} = \left(\frac{\partial h}{\partial T}\right)_\alpha^{-1}\left[\frac{F_2}{F_1} - \left(\frac{\partial h}{\partial \alpha}\right)_T\right]\frac{d\alpha}{d\theta} \qquad (3.14)$$

$$\frac{dv}{d\theta} = -\left[u + \frac{1}{v}\left(\frac{F_2}{F_1}\right)\frac{d\alpha}{d\theta}\right] \qquad (3.15)$$

where

$$F_1 = \frac{[(1-\alpha)Z]^2}{\left(\frac{\partial h}{\partial T}\right)_\alpha}\,\frac{dK_p}{dT} - 4b\alpha^2\rho(1-\alpha)Z \qquad (3.16)$$

$$F_2 = \frac{[(1-\alpha)Z]^2}{\left(\frac{\partial h}{\partial T}\right)_\alpha}\left(\frac{\partial h}{\partial \alpha}\right)_T\frac{dK_p}{dT} + 4b\alpha p[Z + (1-\alpha)] \qquad (3.17)$$

$$F_3 = 1 - R\left[\frac{Z}{\left(\frac{\partial h}{\partial T}\right)_\alpha} + \left(Tb - Z\frac{\left(\frac{\partial h}{\partial \alpha}\right)_T}{\left(\frac{\partial h}{\partial T}\right)_\alpha}\right)\frac{F_1}{F_2}\right] \qquad (3.18)$$

and where p and u are given by the equation of state and by the energy equation, respectively.

3.3 Method of Solution

For the numerical evaluation, the present problem is treated as an inverse one; that is, for a specified shock angle, the associated cone angle results from the calculation. The integration is performed by using a Runge-Kutta technique of fourth-order accuracy with a fixed step size of $2 \cdot 10^{-4}$ radians. The integration proceeds from the shock wave towards the body surface. The cone angle θ_b is determined by finding the angle at which the normal velocity component v vanishes (eq. 2.11). If the solution is desired for a specified cone semi-vertex angle, the calculation is repeated until v vanishes at the specified θ_b. A large number of cases have been calculated, and the results are discussed in section 5.1 of this report.

SECTION IV

NONEQUILIBRIUM FLOW PAST A CIRCULAR CONE

4.1 Governing Equations

In connection with Dorodnitsyn's integral method (Ref. 6), it is convenient to treat the equations of motion in a surface oriented orthogonal coordinate system which is indicated in Fig. 9. It should be noticed that from now on the velocity components in the flow field are defined in a manner which differs from the definition used in section III.

The equations of motion were derived in Ref. 1 for a pointed body of arbitrary convex surface curvature. Without rederiving these equations, they are listed here as they apply for a circular cone which is characterized by the semi-vertex angle θ_b. For convenience, we shall set $\theta_b = \theta$ from now on.

Conservation of mass:

$$\frac{\partial}{\partial x}(\rho u r) + \frac{\partial}{\partial y}(\rho v r) = 0 \tag{4.1}$$

x-Momentum:

$$\frac{\partial}{\partial x}\left[(p + \rho u^2) r\right] + \frac{\partial}{\partial y}(\rho u v r) - p \sin\theta = 0 \tag{4.2}$$

y-Momentum:

$$\frac{\partial}{\partial x}(\rho u v r) + \frac{\partial}{\partial y}\left[(p + \rho v^2) r\right] - p \cos\theta = 0 \tag{4.3}$$

Rate:

$$\frac{\partial}{\partial x}(\rho u \alpha r) + \frac{\partial}{\partial y}(\rho v \alpha r) - \rho r f = 0 \tag{4.4}$$

Additionally there are the energy equation and the equation of state, respectively:

$$\frac{u^2}{2} + \frac{v^2}{2} + h = h_t = \text{const} \tag{4.5}$$

$$p = \rho R Z T \tag{4.6}$$

4.2 Method of Integral Relations

4.2.1 Method in General--First Approximation

The method of integral relations, as developed by Dorodnitsyn (Ref. 6), was described in detail in Ref. 1. Essentially, it permits, through the use of certain assumptions, a transformation of the above given partial differential equations into ordinary differential equations which are then open to numerical integration. Only a short summary will be given here.

After casting all our partial differential equations in divergence form, namely

$$\frac{\partial F_i}{\partial x} + \frac{\partial G_i}{\partial y} + H_i = 0 \qquad (4.7)$$

$$(i = 1, 2, \ldots, m)$$

where x and y are the independent variables, while F_i, G_i and H_i are the known functions of the dependent variables, and assuming that F_i and H_i can be represented by polynomials of the form

$$F_i = \sum_{n=0}^{N} a_{in}(x)\, y^n \qquad (4.8)$$

$$H_i = \sum_{n=0}^{N} b_{in}(x)\, y^n \qquad (4.9)$$

and also dividing the region between the shock and the body surface into N strips of equal width (Fig. 10 shows a two-strip arrangement), eq. (4.7) can be integrated across each strip, which results in a system of $m \cdot N$ ordinary differential equations of the following form:

$$\sum_{n=0}^{N} \frac{1}{n+1} \frac{d}{dx} \left[a_{in}(x) \left(y_{k+1}^{n+1} - y_k^{n+1} \right) \right] - \left[\frac{k+1}{N} F_{i,k+1} - \frac{k}{N} F_{i,k} \right] \frac{dy_s}{dx}$$

$$+ G_{i,k+1} - G_{i,k} + \sum_{n=0}^{N} \frac{b_{in}(x)}{n+1} \left(y_{k+1}^{n+1} - y_k^{n+1} \right) = 0 \qquad (4.10)$$

where $k = 0, 1, \ldots, N-1$; $n = 0, 1, \ldots, N$ and $i = 1, 2, \ldots, m$.

For the first approximation, we have $N = 1$, $k = 0$, $n = 0, 1$. Hence, eq. (4.10) can now be simplified and, for the first approximation, results in

$$\frac{d}{dx}(F_{i,s} + F_{i,b}) - \frac{1}{y_s}(F_{i,s} - F_{i,b})\frac{dy_s}{dx}$$

$$+ \frac{2}{y_s}(G_{i,s} - G_{i,b}) + (H_{i,s} + H_{i,b}) = 0 \tag{4.11}$$

The above equation might be called an operator equation, allowing us to transform our partial differential equations of the form (4.7) directly into ordinary differential equations for the dependent variables along the body surface and along the shock wave.

4.2.2 Second Approximation

For the second approximation, we have $N = 2$, $n = 0, 1, 2$ and $k = 0, 1$. Hence, from eq. (4.8) or (4.9), the polynomial approximation has the general form

$$P_i = c_{i0}(x) + c_{i1}(x)\,y + c_{i2}(x)\,y^2 \tag{4.12}$$

According to Fig. 10, it is found that at

$$\left.\begin{aligned}
y = 0: \quad & P_{i,b} = c_{i0}(x) \\
y = \frac{y_s}{2}: \quad & P_{i,2} = c_{i0}(x) + c_{i1}(x)\frac{y_s}{2} + c_{i2}(x)\frac{y_s^2}{4} \\
y = y_s: \quad & P_{i,s} = c_{i0}(x) + c_{i1}(x)\,y_s + c_{i2}(x)\,y_s^2
\end{aligned}\right\} \tag{4.13}$$

From eq. (4.13), the coefficient functions in general are then

$$\left.\begin{aligned}
c_{i0}(x) &= P_{i,b} \\
c_{i1}(x) &= \frac{1}{y_s}(4P_{i,2} - P_{i,s} - 3P_{i,b}) \\
c_{i2}(x) &= \frac{2}{y_s^2}(P_{i,b} - 2P_{i,2} + P_{i,s})
\end{aligned}\right\} \tag{4.14}$$

Applying this procedure to F_i and H_i, eq. (4.10) can now be simplified; and for the strip between $y = 0$ and $y = y_s/2$, the following equation results:

$$\frac{d}{dx}(5F_{i,b} + 8F_{i,2} - F_{i,s}) + \frac{1}{y_s}(5F_{i,b} - 4F_{i,2} - F_{i,s})\frac{dy_s}{dx}$$
$$+ \frac{24}{y_s}(G_{i,2} - G_{i,b}) + (5H_{i,b} + 8H_{i,2} - H_{i,s}) = 0 \tag{4.15}$$

Similarly, one obtains for the strip between $y = y_s/2$ and $y = y_s$ the following equation:

$$\frac{d}{dx}(8F_{i,2} + 5F_{i,s} - F_{i,b}) + \frac{1}{y_s}(20F_{i,2} - 19F_{i,s} - F_{i,b})\frac{dy_s}{dx}$$
$$+ \frac{24}{y_s}(G_{i,s} - G_{i,2}) + (8H_{i,2} + 5H_{i,s} - H_{i,b}) = 0 \tag{4.16}$$

By properly manipulating eq. (4.15) and (4.16), that is subtracting and adding them in a suitable fashion, the following simpler equations are finally obtained:

$$\frac{d}{dx}(F_{i,b} - F_{i,s}) + \frac{1}{y_s}(F_{i,b} - 4F_{i,2} + 3F_{i,s})\frac{dy_s}{dx}$$
$$- \frac{4}{y_s}(G_{i,b} - 2G_{i,2} + G_{i,s}) + (H_{i,b} - H_{i,s}) = 0 \tag{4.17}$$

$$\frac{d}{dx}(2F_{i,2} + F_{i,s}) + \frac{4}{y_s}(F_{i,2} - F_{i,s})\frac{dy_s}{dx}$$
$$- \frac{1}{y_s}(G_{i,b} + 4G_{i,2} - 5G_{i,s}) + (2H_{i,2} + H_{i,s}) = 0 \tag{4.18}$$

It may be of interest to note that eq. (4.17) and (4.18) are also obtained if the strips are selected such that one strip is bounded by the lines $y = 0$ and $y = y_s/2$, and the other strip is bounded by the lines $y = 0$ and $y = y_s$. Comparing the two-strip analysis with the one-strip analysis, eq. (4.17) and (4.18) correspond to eq. (4.11).

4.2.3 Application of the Second Approximation

Applying now eq. (4.17) and (4.18) to eqs. (4.1) through (4.4), the following set of ordinary differential equations is obtained:

Continuity:

$$\frac{d}{dx}(\rho_b u_b r_b - \rho_s u_s r_s) = \tag{4.19a}$$

$$= \frac{1}{y_s}(4\rho_2 u_2 r_2 - \rho_b u_b r_b - 3\rho_s u_s r_s)\frac{dy_s}{dx} + \frac{4}{y_s}(\rho_s v_s r_s - 2\rho_2 v_2 r_2)$$

$$\frac{d}{dx}(2\rho_2 u_2 r_2 + \rho_s u_s r_s) = \tag{4.19b}$$

$$= \frac{4}{y_s}(\rho_s u_s r_s - \rho_2 u_2 r_2)\frac{dy_s}{dx} + \frac{1}{y_s}(4\rho_2 v_2 r_2 - 5\rho_s v_s r_s)$$

x-Momentum:

$$\frac{d}{dx}\left[(p_b + \rho_b u_b^2)r_b - (p_s + \rho_s u_s^2)r_s\right] =$$

$$= \frac{1}{y_s}\left[4(p_2 + \rho_2 u_2^2)r_2 - (p_b + \rho_b u_b^2)r_b - 3(p_s + \rho_s u_s^2)r_s\right]\frac{dy_s}{dx}$$

$$+ \frac{4}{y_s}(\rho_s u_s v_s r_s - 2\rho_2 u_2 v_2 r_2) + (p_b - p_s)\frac{dr_b}{dx} \tag{4.20a}$$

$$\frac{d}{dx}\left[2(p_2 + \rho_2 u_2^2)r_2 + (p_s + \rho_s u_s^2)r_s\right] =$$

$$= \frac{4}{y_s}\left[(p_s + \rho_s u_s^2)r_s - (p_2 + \rho_2 u_2^2)r_2\right]\frac{dy_s}{dx} + \frac{1}{y_s}(4\rho_2 u_2 v_2 r_2 - 5\rho_s u_s r_s)$$

$$+ (2p_2 + p_s)\frac{dr_b}{dx} \tag{4.20b}$$

y-Momentum:

$$\frac{d}{dx}(\rho_s u_s v_s r_s) = \frac{1}{y_s}(3\rho_s u_s v_s r_s - 4\rho_2 u_2 v_2 r_2)\frac{dy_s}{dx} - \frac{4}{y_s}\left[p_b r_b - 2(p_2 + \rho_2 v_2^2)r_2\right.$$

$$\left. + (p_s + \rho_s v_s^2)r_s\right] - (p_b - p_s)\cos\theta \tag{4.21a}$$

$$\frac{d}{dx}\left(2\rho_2 u_2 v_2 r_2 + \rho_s u_s v_s r_s\right) =$$

$$= \frac{4}{y_s}\left(\rho_s u_s v_s r_s - \rho_2 u_2 v_2 r_2\right)\frac{dy_s}{dx} + \frac{1}{y_s}\left[p_b r_b + 4(p_2 + \rho_2 v_2^2) r_2\right.$$

$$\left. - 5(p_s + \rho_s v_s^2) r_s\right] + (2p_2 + p_s)\cos\theta \tag{4.21b}$$

Rate:

$$\frac{d}{dx}\left(\rho_b u_b \alpha_b r_b - \rho_s u_s \alpha_s r_s\right) =$$

$$= \frac{1}{y_s}\left(4\rho_2 u_2 \alpha_2 r_2 - \rho_b u_b \alpha_b r_b - 3\rho_s u_s \alpha_s r_s\right)\frac{dy_s}{dx}$$

$$+ \frac{4}{y_s}\left(\rho_s v_s \alpha_s r_s - 2\rho_2 v_2 \alpha_2 r_2\right) + \rho_b f_b r_b - \rho_s f_s r_s \tag{4.22a}$$

$$\frac{d}{dx}\left(2\rho_2 u_2 \alpha_2 r_2 + \rho_s u_s \alpha_s r_s\right) =$$

$$= \frac{4}{y_s}\left(\rho_s u_s \alpha_s r_s - \rho_2 u_2 \alpha_2 r_2\right)\frac{dy_s}{dx} + \frac{1}{y_s}\left(4\rho_2 v_2 \alpha_2 r_2 - 5\rho_s v_s \alpha_s r_s\right)$$

$$+ 2\rho_2 f_2 r_2 + \rho_s f_s r_s \tag{4.22b}$$

Before the above eight ordinary differential equations can actually be integrated, a considerable rearrangement is necessary. Also, since they contain more than eight unknowns, some additional relations are needed.

Simple geometry (see Fig. 9) yields

$$r_b = x\sin\theta \tag{4.23}$$

$$r_2 = \frac{x}{2}\sin\theta\,(2 + \delta\cot\theta) \tag{4.24}$$

$$r_s = x\sin\theta\,(1 + \delta\cot\theta) \tag{4.25}$$

where

$$\delta = \frac{y_s}{x} \tag{4.26}$$

Also from geometric considerations one obtains

$$\frac{dy_s}{dx} = \tan\beta \tag{4.27}$$

Differentiating now the first three equations and using the last two, it can be shown that

$$\frac{dr_b}{dx} = \sin\theta \tag{4.28}$$

$$\frac{dr_2}{dx} = \frac{1}{2}\sin\theta\,(2+\cot\theta\,\tan\beta) \tag{4.29}$$

$$\frac{dr_s}{dx} = \sin\theta\,(1+\cot\theta\,\tan\beta) \tag{4.30}$$

Substituting now the expressions which are given in eq. (4.23) through (4.30) into eq. (4.19a) through (4.22b), and rearranging some terms, the following equations result:

Continuity:

$$\frac{d}{dx}(\rho_b u_b) - (1+\delta\cot\theta)\frac{d}{dx}(\rho_s u_s) =$$

$$= \frac{1}{x}\left[\frac{1}{\delta}\left\{[2\rho_2 u_2(2+\delta\cot\theta) - 3\rho_s u_s(1+\delta\cot\theta) - \rho_b u_b]\tan\beta\right.\right.$$

$$\left.\left. + 4[\rho_s v_s(1+\delta\cot\theta) - \rho_2 v_2(2+\delta\cot\theta)]\right\} - \rho_b u_b + \rho_s u_s(1+\cot\theta\tan\beta)\right] \tag{4.31a}$$

$$(2+\delta\cot\theta)\frac{d}{dx}(\rho_2 u_2) + (1+\delta\cot\theta)\frac{d}{dx}(\rho_s u_s) =$$

$$= \frac{1}{x}\left[\frac{1}{\delta}\left\{[4\rho_s u_s(1+\delta\cot\theta) - 2\rho_2 u_2(2+\delta\cot\theta)]\tan\beta + 2\rho_2 v_2(2+\delta\cot\theta)\right.\right.$$

$$\left.\left. - 5\rho_s v_s(1+\delta\cot\theta)\right\} - \rho_2 u_2(2+\cot\theta\tan\beta) - \rho_s u_s(1+\cot\theta\tan\beta)\right] \tag{4.31b}$$

x-Momentum:

$$\frac{d}{dx}(p_b + \rho_b u_b^2) - (1 + \delta \cot\theta)\frac{d}{dx}(p_s + \rho_s u_s^2) =$$

$$= \frac{1}{x}\left[\frac{1}{\delta}\left([2(p_2 + \rho_2 u_2^2)(2 + \delta\cot\theta) - 3(p_s + \rho_s u_s^2)(1 + \delta\cot\theta) - (p_b + \rho_b u_b^2)]\tan\beta + 4[\rho_s u_s v_s(1 + \delta\cot\theta) - \rho_2 u_2 v_2(2 + \delta\cot\theta)]\right) + (p_s + \rho_s u_s^2)(1 + \cot\theta\tan\beta) - p_s - \rho_b u_b^2\right] \tag{4.32a}$$

$$(2 + \delta\cot\theta)\frac{d}{dx}(p_2 + \rho_2 u_2^2) + (1 + \delta\cot\theta)\frac{d}{dx}(p_s + \rho_s u_s^2) =$$

$$= \frac{1}{x}\left[\frac{1}{\delta}\left([4(p_s + \rho_s u_s^2)(1 + \delta\cot\theta) - 2(p_2 + \rho_2 u_2^2)(2 + \delta\cot\theta)]\tan\beta + 2\rho_2 u_2 v_2(2 + \delta\cot\theta) - 5\rho_s u_s v_s(1 + \delta\cot\theta)\right) + 2p_2 + p_s - (p_2 + \rho_2 u_2^2)(2 + \cot\theta\tan\beta) - (p_s + \rho_s u_s^2)(1 + \cot\theta\tan\beta)\right] \tag{4.32b}$$

y-Momentum:

$$(1 + \delta\cot\theta)\frac{d}{dx}(\rho_s u_s v_s) =$$

$$= \frac{1}{x}\left[\frac{1}{\delta}\left([3\rho_s u_s v_s(1 + \delta\cot\theta) - 2\rho_2 u_2 v_2(2 + \delta\cot\theta)]\tan\beta - 4[p_b + (p_s + \rho_s v_s^2)(1 + \delta\cot\theta) - (p_2 + \rho_2 v_2^2)(2 + \delta\cot\theta)]\right) + (p_s - p_b)\cot\theta - \rho_s u_s v_s(1 + \cot\theta\tan\beta)\right] \tag{4.33a}$$

$$(2+\delta \cot\theta)\frac{d}{dx}(\rho_2 u_2 v_2) + (1+\delta\cot\theta)\frac{d}{dx}(\rho_s u_s v_s) =$$

$$= \frac{1}{x}\left[\frac{1}{\delta}\left([2\rho_s u_s v_s(1+\delta\cot\theta) - \rho_2 u_2 v_2(2+\delta\cot\theta)]\ 2\ \tan\beta \right.\right.$$

$$\left. + p_b - 5(p_s + \rho_s v_s^2)(1+\delta\cot\theta) + 2(p_2 + \rho_2 v_2^2)(2+\delta\cot\theta)\right)$$

$$\left. + (2p_2 + p_s)\cot\theta - \rho_s u_s v_s(1+\cot\theta\tan\beta) - \rho_2 u_2 v_2(2+\cot\theta\tan\beta)\right] \qquad (4.33b)$$

Rate:

$$\frac{d}{dx}(\rho_b u_b \alpha_b) - (1+\delta\cot\theta)\frac{d}{dx}(\rho_s u_s \alpha_s) =$$

$$= \frac{1}{x}\left[\frac{1}{\delta}\left([2\rho_2 u_2 \alpha_2(2+\delta\cot\theta) - 3\rho_s u_s \alpha_s(1+\delta\cot\theta) - \rho_b u_b \alpha_b]\tan\beta \right.\right.$$

$$\left. + 4[\rho_s v_s \alpha_s(1+\delta\cot\theta) - \rho_2 v_2 \alpha_2(2+\delta\cot\theta)]\right)$$

$$\left. + \rho_s u_s \alpha_s(1+\cot\theta\tan\beta) - \rho_b u_b \alpha_b\right] + \rho_b f_b - \rho_s f_s(1+\delta\cot\theta) \qquad (4.34a)$$

$$(2+\delta\cot\theta)\frac{d}{dx}(\rho_2 u_2 \alpha_2) + (1+\delta\cot\theta)\frac{d}{dx}(\rho_s u_s \alpha_s) =$$

$$= \frac{1}{x}\left[\frac{1}{\delta}\left([2\rho_s u_s \alpha_s(1+\delta\cot\theta) - \rho_2 u_2 \alpha_2(2+\delta\cot\theta)]\ 2\tan\beta \right.\right.$$

$$\left. + 2\rho_2 v_2 \alpha_2(2+\delta\cot\theta) - 5\rho_s v_s \alpha_s(1+\delta\cot\theta)\right) - \rho_2 u_2 \alpha_2(2+\cot\theta\tan\beta)$$

$$\left. - \rho_s u_s \alpha_s(1+\cot\theta\tan\beta)\right] + \rho_2 f_2(2+\delta\cot\theta) + \rho_s f_s(1+\delta\cot\theta) \qquad (4.34b)$$

Considering that all variables on the downstream side of the shock wave (subscript s) and their gradients can be expressed as functions of the shock wave angle σ (see Appendix B), eq. (4.27) together with the above eight equations form a system of nine differential equations for thirteen unknowns. Additional differential equations are obtained by differentiating the energy equation and the equation of state and applying them at the body surface (subscript b) and at the strip interface (subscript 2). Hence, from the energy equation,

$$u_2 \frac{du_2}{dx} + v_2 \frac{dv_2}{dx} + S_2 \frac{dT_2}{dx} + L_2 \frac{d\alpha_2}{dx} = 0 \tag{4.35}$$

$$u_b \frac{du_b}{dx} + S_b \frac{dT_b}{dx} + L_b \frac{d\alpha_b}{dx} = 0 \tag{4.36}$$

where

$$S = \left(\frac{\partial h}{\partial T}\right)_\alpha$$

$$L = \left(\frac{\partial h}{\partial \alpha}\right)_T$$

and from the equation of state

$$\frac{1}{p_2} \frac{dp_2}{dx} = \frac{1}{\rho_2} \frac{d\rho_2}{dx} + \frac{1}{T_2} \frac{dT_2}{dx} + \frac{b}{Z_2} \frac{d\alpha_2}{dx} \tag{4.37}$$

$$\frac{1}{p_b} \frac{dp_b}{dx} = \frac{1}{\rho_b} \frac{d\rho_b}{dx} + \frac{1}{T_b} \frac{dT_b}{dx} + \frac{b}{Z_b} \frac{d\alpha_b}{dx} \tag{4.38}$$

Now eq. (4.27) and eq. (4.31a) through eq. (4.38) constitute a system of thirteen differential equations which can be solved for the following thirteen unknowns:

at body surface: $\rho_b, T_b, \alpha_b, p_b, u_b$

at strip interface: $\rho_2, T_2, \alpha_2, p_2, u_2, v_2$

at shock: σ, y_s .

By using the last four equations to eliminate the derivations of $u_b, u_2, p_b,$ and p_2 from eq. (4.31a) through (4.34b), the latter equations yield a system of eight equations in the unknown gradients of the eight variables $\rho_b, T_b, \alpha_b, \rho_2, T_2, \alpha_2, v_2,$ and σ, which is given on the following page.

$$a_{11}\frac{d\rho_b}{dx} + a_{12}\frac{dT_b}{dx} + a_{13}\frac{d\alpha_b}{dx} + a_{18}\frac{d\sigma}{dx} = A_1 \quad (4.39)$$

$$a_{24}\frac{d\rho_2}{dx} + a_{25}\frac{dT_2}{dx} + a_{26}\frac{d\alpha_2}{dx} + a_{27}\frac{dv_2}{dx} + a_{28}\frac{d\sigma}{dx} = A_2 \quad (4.40)$$

$$a_{31}\frac{d\rho_b}{dx} + a_{32}\frac{dT_b}{dx} + a_{33}\frac{d\alpha_b}{dx} + a_{38}\frac{d\sigma}{dx} = A_3 \quad (4.41)$$

$$a_{44}\frac{d\rho_2}{dx} + a_{45}\frac{dT_2}{dx} + a_{46}\frac{d\alpha_2}{dx} + a_{47}\frac{dv_2}{dx} + a_{48}\frac{d\sigma}{dx} = A_4 \quad (4.42)$$

$$a_{58}\frac{d\sigma}{dx} = A_5 \quad (4.43)$$

$$a_{64}\frac{d\rho_2}{dx} + a_{65}\frac{dT_2}{dx} + a_{66}\frac{d\alpha_2}{dx} + a_{67}\frac{dv_2}{dx} + a_{68}\frac{d\sigma}{dx} = A_6 \quad (4.44)$$

$$a_{71}\frac{d\rho_b}{dx} + a_{72}\frac{dT_b}{dx} + a_{73}\frac{d\alpha_b}{dx} + a_{78}\frac{d\sigma}{dx} = A_7 \quad (4.45)$$

$$a_{84}\frac{d\rho_2}{dx} + a_{85}\frac{dT_2}{dx} + a_{86}\frac{d\alpha_2}{dx} + a_{87}\frac{dv_2}{dx} + a_{88}\frac{d\sigma}{dx} = A_8 \quad (4.46)$$

The a_{ij} and A_i are given in Appendix C.

These eight equations are, respectively, two continuity, two x-momentum, two y-momentum, and two rate equations. It can be seen that due to the y-momentum equation (4.43), containing the gradient of σ only, the system of eight equations can be broken up into two sets of equations, each group consisting of one continuity, x-momentum, y-momentum, and rate equation. Once these two sets are solved, u_b, u_2, p_b, and p_2 are calculated from the energy equation and from the equation of state directly.

4.3 Method of Solution

4.3.1 Initial Values--Frozen Flow

In order to start the numerical integration of the system (4.39) through (4.46), the values of all variables must be known at the cone tip ($x = 0$). The use of frozen shock conditions implies that the flow is frozen at the tip of the cone. Therefore, the frozen flow values serve as initial values.

For frozen flow, just as for perfect gas flow, there is a conical attached shock wave. By definition, then also the interface is a conical surface. Hence, using the well-known assumption that all variables are constant on coaxial conical surfaces having the same vertex as the conical body (see section 3.1), one can set

$$\frac{dg_s}{dx} = \frac{dg_2}{dx} = \frac{dg_b}{dx} = 0 \tag{4.47}$$

where g stands for any of the flow variables. Since also

$$\lim_{x \to 0} \delta = \lim_{x \to 0} \left(\frac{y_s}{x} \right) = \tan \beta \tag{4.48}$$

eq. (4.31a) through (4.34b) reduce to nonlinear algebraic equations which can be brought into the following form:

Continuity:

$$\rho_2(u_2 - 2v_2 \cot \beta)(2 + \cot \theta \tan \beta) - \rho_b u_b = \rho_s(u_s - 2v_s \cot \beta)(1 + \cot \theta \tan \beta) \tag{4.49}$$

$$\rho_2(3u_2 - 2v_2 \cot \beta)(2 + \cot \theta \tan \beta) = \rho_s(3u_s - 5v_s \cot \beta)(1 + \cot \theta \tan \beta) \tag{4.50}$$

x-Momentum:

$$(p_b - p_s) - 2(p_2 - p_s)(2 + \cot\theta\tan\beta) + 2\rho_b u_b^2 = 2\rho_2 u_2(u_2$$

$$- 2v_2 \cot\beta)(2 + \cot\theta\tan\beta) - 2\rho_s u_s(u_s - 2v_s \cot\beta)(1 + \cot\theta\tan\beta) \tag{4.51}$$

$$(p_2 - p_s)(4 + 3\cot\theta\tan\beta) = \rho_s u_s(3u_s - 5v_s\cot\beta)(1 + \cot\theta\tan\beta)$$

$$- \rho_2 u_2(3u_2 - 2v_2\cot\beta)(2 + \cot\theta\tan\beta) \tag{4.52}$$

y-Momentum:

$$4(p_2 - p_s)(\cot\theta + 2\cot\beta) - (p_b - p_s)(\cot\theta + 4\cot\beta) =$$

$$= 2\rho_2 v_2(u_2 - 2v_2\cot\beta)(2 + \cot\theta\tan\beta)$$

$$- 2\rho_s v_s(u_s - 2v_s\cot\beta)(1 + \cot\theta\tan\beta) \tag{4.53}$$

$$(p_b - p_s)\cot\beta + 4(p_2 - p_s)(\cot\theta + \cot\beta) = \rho_2 v_2(3u_2 - 2v_2\cot\beta)(2$$

$$+ \cot\theta\tan\beta) - \rho_s v_s(3u_s - 5v_s\cot\beta)(1 + \cot\theta\tan\beta) \tag{4.54}$$

Rate:

$$\rho_2\alpha_2(u_2 - 2v_2\cot\beta)(2 + \cot\theta\tan\beta) - \rho_b u_b \alpha_b = \rho_s\alpha_s(u_s$$

$$- 2v_s\cot\beta)(1 + \cot\theta\tan\beta) \tag{4.55}$$

$$\rho_2\alpha_2(3u_2 - 2v_2\cot\beta)(2 + \cot\theta\tan\beta) =$$

$$= \rho_s\alpha_s(3u_s - 5v_s\cot\beta)(1 + \cot\theta\tan\beta) \tag{4.56}$$

The above equations can also be obtained by formally multiplying eq. (4.31a) through (4.34b) by x, and then taking the limit for $x \rightarrow 0$.

It is noticed that eq. (4.55) and (4.56) still contain α_b, α_2, and α_s, although these equations were derived by assuming frozen flow. It will now be shown that, in fact, $\alpha_b = \alpha_2 = \alpha_s$, which means that the conditions for frozen flow are satisfied.

Solving eq. (4.56) for α_2, one obtains

$$\alpha_2 = \left[\frac{\rho_s(3u_s - 5v_s \cot\beta)(1 + \cot\theta \tan\beta)}{\rho_2(3u_2 - 2v_2 \cot\beta)(2 + \cot\theta \tan\beta)} \right] \alpha_s \tag{4.57}$$

Since it can be seen from eq. (4.50) that the square bracket term in eq. (4.57) is equal to unity, it is shown that

$$\alpha_2 = \alpha_s \tag{4.58}$$

Due to eq. (4.58), α_2 in eq. (4.55) can now be replaced by α_s, hence

$$\alpha_b = \frac{\alpha_s}{\rho_b u_b} \Big[\rho_2(u_2 - 2v_2 \cot\beta)(2 + \cot\theta \tan\beta) - \rho_s(u_s - 2v_s \cot\beta)(1 + \cot\theta \tan\beta) \Big] \tag{4.59}$$

Eq. (4.49) shows that the square bracket in eq. (4.59) is equal to $(\rho_b u_b)$ hence

$$\alpha_b = \alpha_s \tag{4.60}$$

Consequently, due to the boundary conditions (section 2.2), and due to eq. (4.58) and (4.60), the condition for frozen flow

$$\alpha_b = \alpha_2 = \alpha_s = \alpha_1 \tag{4.61}$$

is satisfied.

Due to the nonlinearity of the equations, a trial and error procedure must be used to calculate the remaining flow variables for frozen flow. It seems to be convenient to calculate the interface conditions first. It is found that eq. (4.50) and eq. (4.52) do not contain any body surface variables.

Eliminating the body surface pressure from the two y-momentum equations, a third equation which contains interface and shock values only is available. Combining these three equations with the equation of state and the energy equation, there are five equations for the five unknowns: ρ_2, T_2, p_2, u_2, and v_2.

The first step is to combine eq. (4.52) and the two y-momentum equations in order to eliminate p_s, p_b, and p_2. The result is an equation in ρ_2, u_2, and v_2. Combining this equation with eq. (4.50) in order to eliminate u_2 or v_2, a quadratic equation for either v_2 or u_2 can be obtained. Eliminating u_2, the quadratic equation for v_2 is

$$8A\rho_2 \cot\beta\, v_2^2 - \rho_s(3u_s - 5v_s \cot\beta)(8B + 14 + 3\cot\theta \tan\beta)\, v_2 + \rho_s\Big[6v_s(u_s - 2v_s\cot\beta) + (3u_s - 5v_s\cot\beta)\Big\{3v_s(4 + \cot\theta\tan\beta) - 4B\tan\beta\Big[\frac{\rho_s}{\rho_2}(3u_s - 5v_s\cot\beta)A - 3u_s\Big]\Big\}\Big] = 0 \qquad (4.62)$$

where

$$A = \frac{2 + \cot\theta \tan\beta}{1 + \cot\theta \tan\beta} \qquad (4.63)$$

$$B = \frac{6\cot^2\beta + 6\cot\theta\cot\beta + \cot^2\theta}{4 + 3\cot\theta\tan\beta} \qquad (4.64)$$

Assuming a value for σ and ρ_2, where $\rho_s < \rho_2 < \rho_b$ (and ρ_b is known from the first approximation), eq. (4.62) can be solved for v_2. Since there are two solutions, the correct solution must be selected such that $0 \leq |v_2| \leq |v_s|$. Knowing v_2, one obtains from eq. (4.50)

$$u_2 = \frac{1}{3}\left[\frac{\rho_s}{\rho_2}(3u_s - 5v_s\cot\beta)\frac{1 + \cot\theta\tan\beta}{2 + \cot\theta\tan\beta} + 2v_2\cot\beta\right] \qquad (4.65)$$

and from eq. (4.50) and (4.52):

$$p_2 = \rho_s(3u_s - 5v_s \cot\beta)\frac{1 + \cot\theta \tan\beta}{4 + 3\cot\theta \tan\beta}(u_s - u_2) + p_s \tag{4.66}$$

From the equation of state

$$T_2 = \frac{p_2}{\rho_2 RZ} \tag{4.67}$$

Having assumed ρ_2, and having calculated T_2 as function of u_2 and v_2, there remains the energy equation for a check on ρ_2

$$u_2^2 + v_2^2 = 2(h_t - h_2) \tag{4.68}$$

If the energy equation is not satisfied, a new value of ρ_2 has to be assumed. The calculation must then be repeated until a consistent set of values of all variables at the interface is found.

With the values at the interface calculated, the body surface variables are determined from the remaining equations. Eq. (4.49), (4.51), and (4.54) can be combined in order to eliminate p_b and ρ_b. The resulting equation can be solved for the body surface velocity as follows:

$$u_b = u_2 + \Big[\rho_s(1 + \cot\theta \tan\beta)\,[\,(v_2 - v_s)(3u_s - 5v_s \cot\beta) - 2(u_2 - u_s)(u_s - 2v_s \cot\beta)\cot\beta\,] - 2(p_2 - p_s)\cot\beta(4 + 3\cot\theta\tan\beta)\Big]\Big[\,2\cot\beta\,[\,\rho_s(u_s - 2v_s \cot\beta)(1 + \cot\theta \tan\beta) - \rho_2(u_2 - 2v_2\cot\beta)(2 + \cot\theta\tan\beta)\,]\Big]^{-1} \tag{4.69}$$

Solving eq. (4.49) for the surface density, the latter one is

$$\rho_b = \frac{1}{u_b}\,[\,\rho_2(u_2 - 2v_2 \cot\beta)(2 + \cot\theta \tan\beta) - \rho_s(u_s - 2v_s \cot\beta)(1 + \cot\theta \tan\beta)\,] \tag{4.70}$$

From the y-momentum equation, eq. (4.54), and the continuity equation, eq. (4.50), the surface pressure becomes

$$p_b = p_s + (1 + \cot\theta \tan\beta)\Big[\rho_s(v_2 - v_s)(3u_s - 5v_s \cot\beta)$$

$$- 4(p_2 - p_s)\cot\beta\Big]\tan\beta \qquad (4.71)$$

From the equation of state

$$T_b = \frac{p_b}{\rho_b RZ} \qquad (4.72)$$

Since the above calculations are still based on an assumed value of the shock wave angle σ, the energy equation is now used to verify this assumption. T_b and u_b, as calculated above, have to satisfy the relation

$$u_b^2 = 2(h_t - h_b) \qquad (4.73)$$

If eq. (4.73) is not satisfied, a new value of σ is chosen. The calculation must be repeated by starting with eq. (4.62).

4.3.2 Initial Derivatives

The necessity for determining the derivatives of all variables at $x = 0$ arises from the fact that for the initial values, which were calculated in the previous section, the system of eq. (4.39) through (4.46) becomes indeterminate. The reason for this, of course, is the direct relation of the algebraic equations (4.49) through (4.56) with the nonhomogeneous terms in the system (4.39) through (4.46), respectively.

However, a set of linear equations for the initial derivatives can be derived from the system (4.39) through (4.46). The indeterminancy can be resolved by applying L'Hospital's rule to the A_i ($i = 1, 2, \ldots, 8$) in order to find their limiting expressions for $x \rightarrow 0$. The resulting equations for the initial gradients are given on the following page.

$$b_{11}\frac{d\rho_b}{dx} + b_{12}\frac{dT_b}{dx} + b_{13}\frac{d\alpha_b}{dx} + b_{14}\frac{d\rho_2}{dx} + b_{15}\frac{dT_2}{dx} + b_{16}\frac{d\alpha_2}{dx} + b_{17}\frac{dv_2}{dx} + b_{18}\frac{d\sigma}{dx} = 0 \tag{4.74}$$

$$b_{24}\frac{d\rho_2}{dx} + b_{25}\frac{dT_2}{dx} + b_{26}\frac{d\alpha_2}{dx} + b_{27}\frac{dv_2}{dx} + b_{28}\frac{d\sigma}{dx} = 0 \tag{4.75}$$

$$b_{31}\frac{d\rho_b}{dx} + b_{32}\frac{dT_b}{dx} + b_{33}\frac{d\alpha_b}{dx} + b_{34}\frac{d\rho_2}{dx} + b_{35}\frac{dT_2}{dx} + b_{36}\frac{d\alpha_2}{dx} + b_{37}\frac{dv_2}{dx} + b_{38}\frac{d\sigma}{dx} = 0 \tag{4.76}$$

$$b_{44}\frac{d\rho_2}{dx} + b_{45}\frac{dT_2}{dx} + b_{46}\frac{d\alpha_2}{dx} + b_{47}\frac{dv_2}{dx} + b_{48}\frac{d\sigma}{dx} = 0 \tag{4.77}$$

$$b_{51}\frac{d\rho_b}{dx} + b_{52}\frac{dT_b}{dx} + b_{53}\frac{d\alpha_b}{dx} + b_{54}\frac{d\rho_2}{dx} + b_{55}\frac{dT_2}{dx} + b_{56}\frac{d\alpha_2}{dx} + b_{57}\frac{dv_2}{dx} + b_{58}\frac{d\sigma}{dx} = 0 \tag{4.78}$$

$$b_{61}\frac{d\rho_b}{dx} + b_{62}\frac{dT_b}{dx} + b_{63}\frac{d\alpha_b}{dx} + b_{64}\frac{d\rho_2}{dx} + b_{65}\frac{dT_2}{dx} + b_{66}\frac{d\alpha_2}{dx} + b_{67}\frac{dv_2}{dx} + b_{68}\frac{d\sigma}{dx} = 0 \tag{4.79}$$

$$b_{71}\frac{d\rho_b}{dx} + b_{72}\frac{dT_b}{dx} + b_{73}\frac{d\alpha_b}{dx} + b_{74}\frac{d\rho_2}{dx} + b_{75}\frac{dT_2}{dx} + b_{76}\frac{d\alpha_2}{dx} + b_{77}\frac{dv_2}{dx} + b_{78}\frac{d\sigma}{dx} = B_7 \tag{4.80}$$

$$b_{84}\frac{d\rho_2}{dx} + b_{85}\frac{dT_2}{dx} + b_{86}\frac{d\alpha_2}{dx} + b_{87}\frac{dv_2}{dx} + b_{88}\frac{d\sigma}{dx} = B_8 \tag{4.81}$$

The b_{ij} and the B_i are given in Appendix D.

4.3.3 Numerical Procedure

For the numerical evaluation, all variables and the coordinates were nondimensionalized as follows:

$$u', v' = \frac{u, v}{u_1} \; ; \qquad p' = \frac{p}{\rho_1 u_1^2} \; ; \qquad \rho' = \frac{\rho}{\rho_1} \; ;$$

$$T' = \frac{T}{T_1} \; ; \qquad h' = \frac{h}{u_1^2} \; ; \qquad R' = \frac{RT_1}{u_1^2} \; ;$$

$$\xi, \eta = \frac{x, y}{l} \; , \quad \text{where} \quad l = \left(\frac{u_b}{f_b}\right)_{x=0} \; ;$$

The equations were then programmed in dimensionless form; all calculations were performed on the UNIVAC 1107 high speed digital computer.

In order to facilitate the numerical evaluation, the problem was programmed in two parts. The first part considers the calculation of the initial values, while the second part is concerned with the integration along the body surface. The calculation starts by evaluating the conditions behind the attached shock wave for a given configuration and an assumed shock wave angle σ, as described in detail in Ref. 1. Knowing the shock wave conditions, the variables at the interface and at the body surface are evaluated as described in section 4.3.1 of the present report. As it was mentioned there, the nonlinear character of the pertinent equations necessitates the use of a trial and error procedure in order to obtain the initial conditions at the interface and at the body surface.

Having completed this first part, initial gradients can be calculated by resolving the system (4.74) through (4.81). With initial values and initial gradients available, the flow conditions at some finite $\Delta\xi$ can be calculated. From this point on, the computation switches over to the system (4.39) through (4.46). This system is then evaluated by a program which mainly uses two subroutines, namely a linear equation solver, and a Runge-Kutta integration technique of fourth-order accuracy. The step size is essentially fixed; however, it can be varied in intervals.

SECTION V

DISCUSSION OF RESULTS

5.1 Equilibrium Flow

Results were obtained for free stream Mach numbers ranging from 10 to 25 and for shock wave angles ranging from 20 to 50 degrees. The free stream temperature and the free stream pressure were fixed at $T_1 = 273.16^{\circ}K$, and at $p_1 = 1.01325 \cdot 10^{-3}$ bar (= 10^{-3} atm), respectively.

For simplicity and generality, the results were correlated on the basis of the hypersonic similarity parameter $M_1 \sin\theta_b$. This correlation was first proposed and used by Romig (Ref. 5) and is very good indeed.

The results from the present investigation are compared with results previously obtained with the method of integral relations (Ref. 1) and with results obtained by Romig (Ref. 5). When comparing the graphs, it should be considered that the present results and those of Ref. 1 are based on the same air model. While Romig basically used the same equations as those in the present analysis, the thermodynamic data were not directly calculated but were taken from more elaborate tables.

It can be seen from Fig. 3 through Fig. 8 that the agreement of the present results with those obtained with the integral method is excellent. With the exception of the surface pressure, the integral method values of which are uniformly about two per cent below the values from the present Taylor-Maccoll type analysis, there is no measurable difference in the results from the two methods. Hence, any deviation of the present results from those of Romig (Ref. 5) can safely be attributed to the difference in the thermodynamic data input.

5.2 Nonequilibrium Flow

Within the time which was allotted to this contract, it was not possible to calculate a large number of cases. However, some results for chemical nonequilibrium flow are presented in Fig. 11 through 18. The case for zero free stream dissociation corresponds to a flight Mach number of $M_1 = 20$ at 40 km geometric altitude. For the second case discussed, the free stream dissociation was arbitrarily taken to be $\alpha_1 = 0.5$, leaving all other free stream parameters unchanged. As a matter of fact, these are the same cases which were already discussed in Ref. 1. The solution of the two-strip integral approximation was just added to the existing figures.

Just as the semi-exact procedure and the standard one-strip approximation (Ref. 1), the two-strip approximation exhibits bounded oscillations of the solution near the cone tip ($x = 0$). The previously successfully used procedure of selecting a relatively large initial step in order to eliminate or by-pass these oscillations was unsuccessful for the present cases. Various combinations of step sizes were tried, and the result is shown in Fig. 11. It is noted that the oscillations have a very distinct pattern which is rather independent of the initial step size. The amplitude is in all cases less than 0.1% of the initial value. What is more important, the solution always converges after the oscillations have died, provided the initial step size is kept below a certain maximum. In our case, this maximum value seems to be around $\xi = 5.0 \cdot 10^{-4}$, as can be seen from Fig. 11.

It may also be mentioned that some results were obtained by using a Runge-Kutta integration technique of third-order accuracy. No difference was found between the solution produced by this technique and a solution using the fourth-order integration technique. The advantage of the third-order accuracy technique then consists of a considerable shorter run time on the computer.

Fig. 12 and 13 show the variation of the shock wave angle and the cone surface velocity with distance from the cone tip. As in all the other figures, the x-coordinate was nondimensionalized by the relaxation length at $x = 0$. Except for the shock wave angle in the case with free stream dissociation, the two-strip solution is, for a sufficiently large distance away from the tip, closer to the equilibrium flow solution than the one-strip solution is. In contrast to the variation of the remaining variables (p_b,

ρ_b, α_b, and T_b), for the shock wave angle σ and the surface velocity u_b, the semi-exact procedure seems to yield a solution which does not appraoch the equilibrium flow solution as well as in the case of the standard one-strip or the two-strip solution. However, it should be kept in mind that all three methods give results which are, for large enough x, well within 1% of the equilibrium flow solution. Numerical calculations are, by their very nature, subject to a certain error; and it may not be wise in this case to rate any particular solution higher than the other one since all of them fall very close together. In other words, they are all believed to be correct within the limits of probable errors due to the numerical integration.

The pressure distribution along the cone surface is shown in Fig. 14. A peak at the cone tip is followed by a drastic drop, and after a slight overexpansion the pressure stays nearly constant along the surface. The two-strip solution is closer to the equilibrium flow solution than the one-strip solution is, but still not as close as the semi-exact solution. But again, all three solutions are very close together.

The surface density and the degree of dissociation along the cone surface, shown in Fig. 15 and 16, respectively, exhibit very similar distributions. Clearly, for large x, the semi-exact solution is closest to the equilibrium solution. Neither the standard one-strip nor the two-strip solution is as good in this sense. It is of particular interest to compare Fig. 16 of this report with Fig. 9 of Ref. 3. There the variation of the vibrational excitation along the surface of a wedge is shown. As one would expect, the general behavior of the degree of vibrational excitation is very similar to the one of the degree of dissociation in the present case of the flow past a cone.

The surface temperature is presented in Fig. 17. While for large x the one-strip solution undershoots the equilibrium solution, the two-strip solution yields temperatures which are higher than for equilibrium flow.

Finally, in Fig. 18 the nonequilibrium shock layer thickness, obtained from the semi-exact, standard one-strip and two-strip methods, are compared with the frozen flow and the equilibrium flow solutions. It is observed that for all nonequilibrium flow calculations the shock wave starts with the same angle as for frozen flow. Farther downstream from the tip, the nonequilibrium flow shock wave is always bracketed by the frozen shock wave on the outside and by the equilibrium shock wave on the inside.

5.3 Conclusions

First, equilibrium flow of dissociating air past a circular cone has been calculated by integrating Taylor-Maccoll's equations. The results were compared with those of previous calculations using Dorodnitsyn's method of integral relations and also with Romig's results. The following conclusions can be drawn:

1) The Taylor-Maccoll analysis yields the same results as the method of integral relations. Both procedures use iterative schemes in order to produce a solution for a particular cone semi-vertex angle.

2) A comparison of the present results with those of Romig confirms the excellent agreement of the simplified air model, used in Ref. 1 and in this report, with more detailed and, therefore, more complex air models.

3) As far as inviscid flow is concerned, the method of calculation presented in this report is applicable for any flight configuration where $M_1 \sin\theta_b \leq 12$.

Second, nonequilibrium hypersonic flow of air has been calculated by using the two-strip integral method and considering nonequilibrium dissociation of oxygen. The present results were compared with solutions previously obtained by using the standard one-strip method and a one-strip semi-exact procedure. The following conclusions can be drawn:

1) In the present application, the two-strip integral method yields a solution which is better than the one-strip solution in the sense that, for large distances away from the tip, the two-strip solution approaches the equilibrium solution closer than the one-strip solution does.

2) In general, under the same flight conditions, the one-strip semi-exact procedure (Ref. 1) yields results which are still closer to the equilibrium solution than either the standard one-strip or the two-strip solution. This is important if the tremendous amount of work is considered which was necessary in order to produce in particular the equations for the two-strip approximation.

3) It was found that the solution obtained from the two-strip integral method exhibits the same bounded oscillations near the tip of the cone which were previously observed in the standard one-strip method and in the semi-exact procedure. For a proper arrangement of the integration step sizes, these oscillations do not seem to have any measurable influence on the solution. Nevertheless, it is recommended that additional studies be undertaken in order to find a proper procedure to eliminate these oscillations.

REFERENCES

1. Thoenes, J., "Inviscid High Temperature Hypersonic Flow of Air Past Pointed Bodies of Revolution," Final Technical Report on Contract No. DA-01-009-AMC-166(Z), University of Alabama Research Institute, Research Report No. 25, May 1965.

2. Taylor, G. I., and Maccoll, J. W., "The Air Pressure on a Cone Moving at High Speeds," Proceedings of the Roayl Society of London, Series A, Vol. 139, March 1933.

3. South, Jerry C., "Application of the Method of Integral Relations to Supersonic Nonequilibrium Flow Past Wedges and Cones," NASA TR R-205, August 1964.

4. Busemann, A., "Drücke auf kegelförmige Spitzen bei Bewegung mit Überschallgeschwindigkeit," Zeitschrift für Angewandte Mathematik und Mechanik, Band 9, pp. 496-498, Berlin 1929.

5. Romig, M. F., "Conical Flow Parameters For Air in Dissociation Equilibrium," Convair Scientific Research Laboratory, Research Report 7, May 1960.

6. Dorodnitsyn, A. A., "A Contribution to the Solution of Mixed Problems of Transonic Aerodynamics," Advances in Aeronautical Sciences, Vol. 2, Pergamon Press, New York, 1959, pp. 832-844.

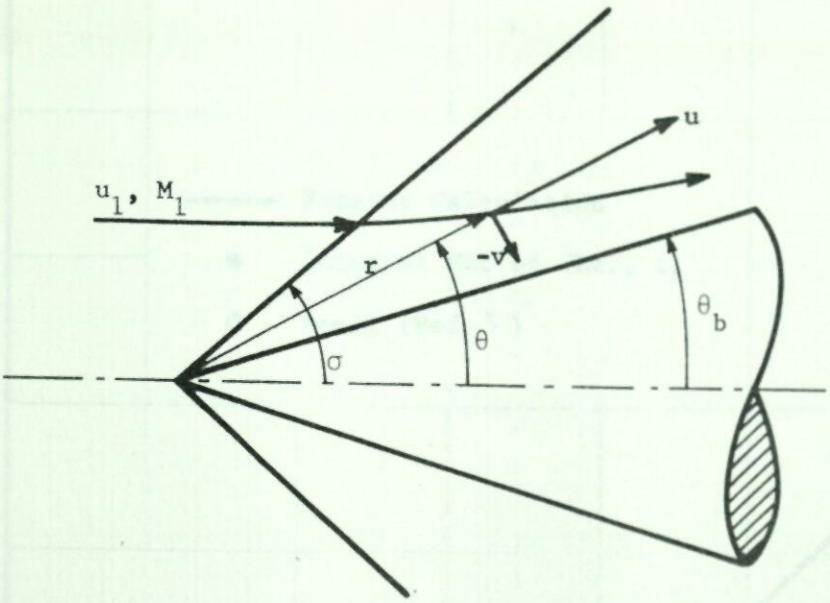

Fig. 1 Flow Geometry on Circular Cone

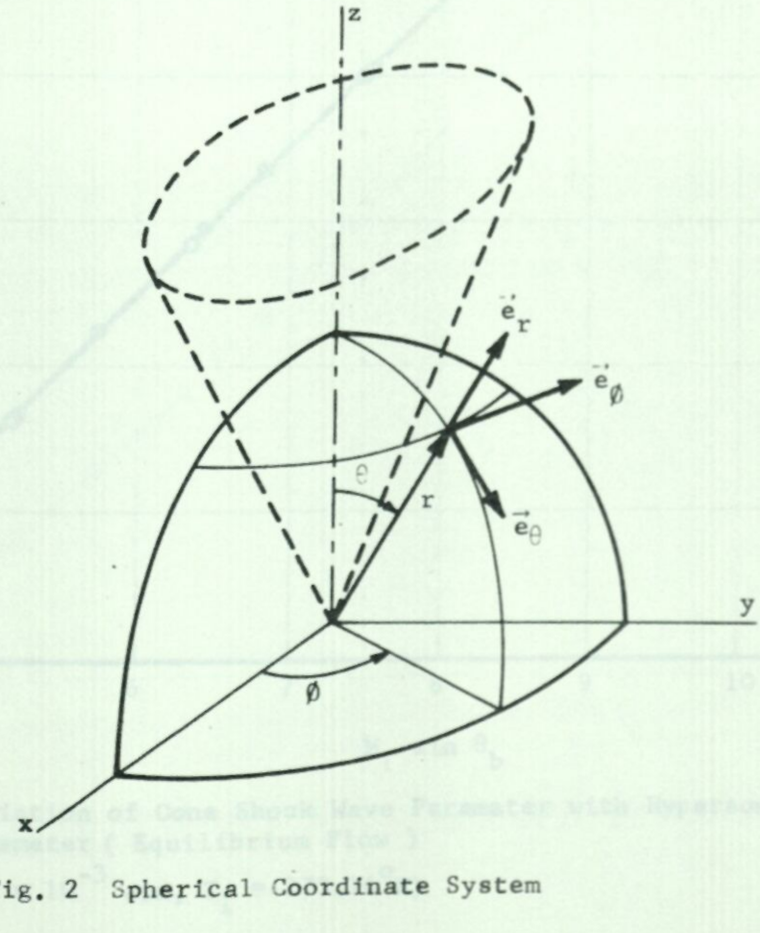

Fig. 2 Spherical Coordinate System

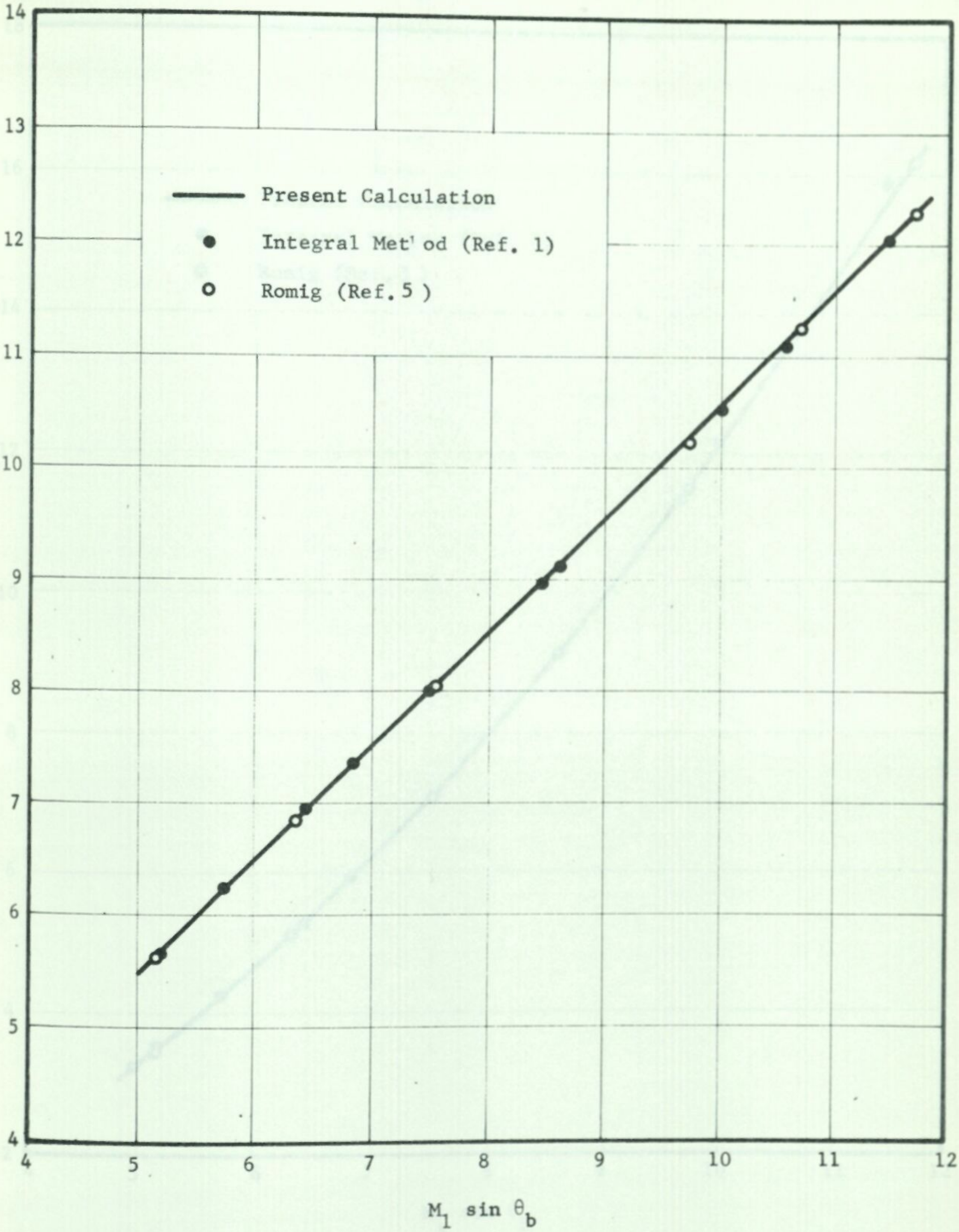

Fig. 3 Variation of Cone Shock Wave Parameter with Hypersonic Similarity Parameter (Equilibrium Flow)

($p_1 = 10^{-3}$ atm, $T_1 = 273.16^{o}K$)

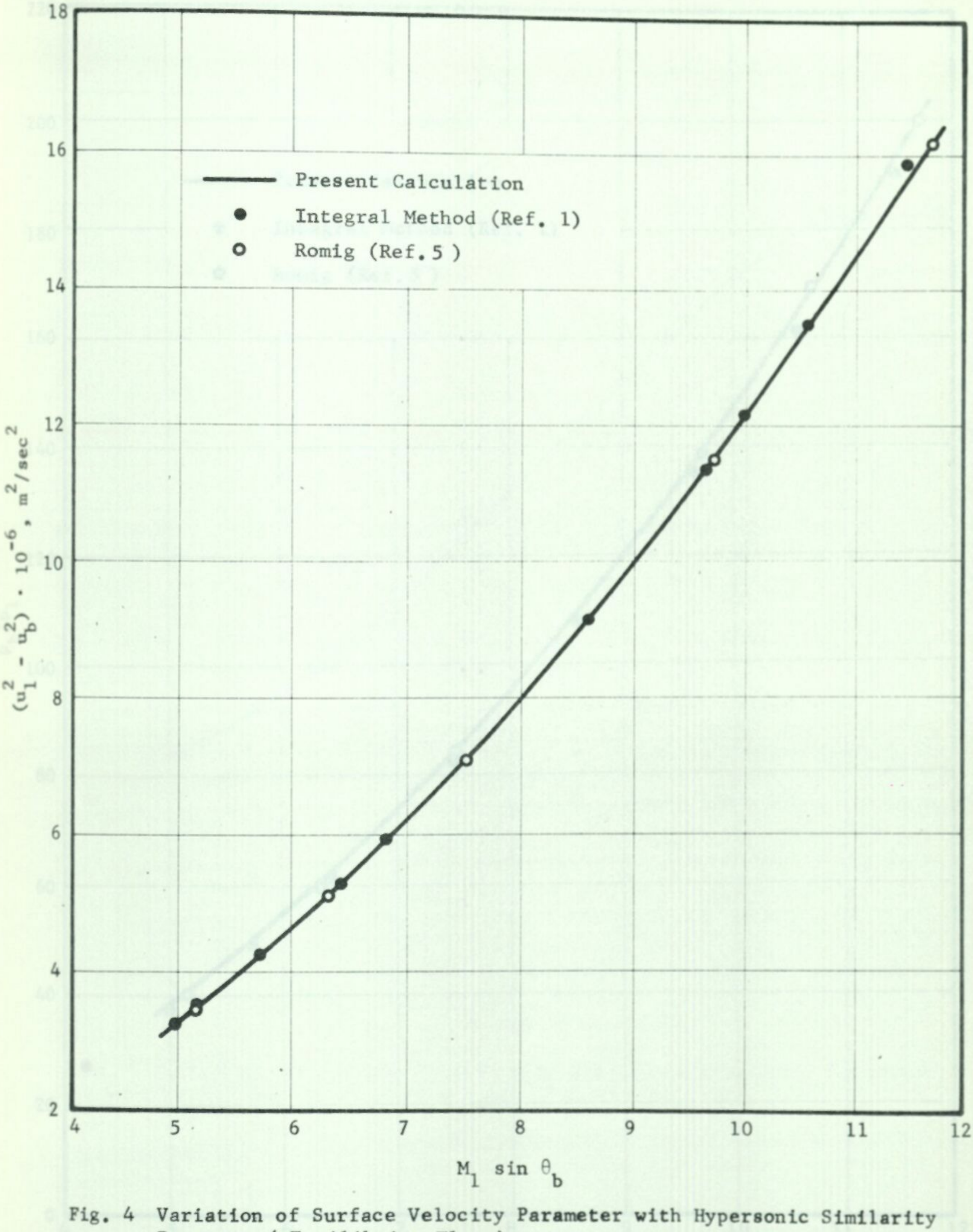

Fig. 4 Variation of Surface Velocity Parameter with Hypersonic Similarity Parameter (Equilibrium Flow)
($p_1 = 10^{-3}$ atm, $T_1 = 273.16^{o}K$)

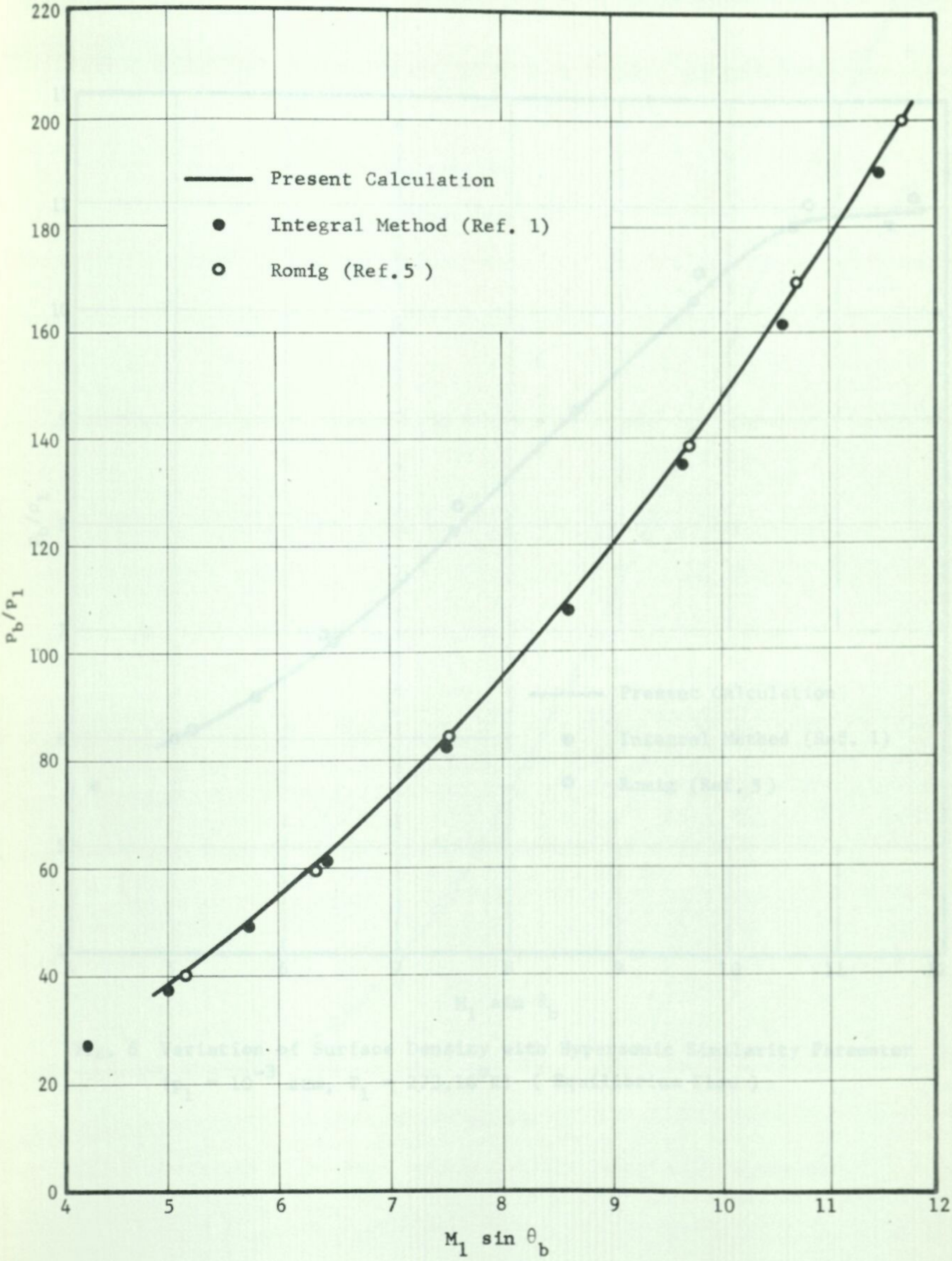

Fig. 5 Variation of Surface Pressure with Hypersonic Similarity Parameter ($p_1 = 10^{-3}$ atm, $T_1 = 273.16^{o}K$) (Equilibrium Flow)

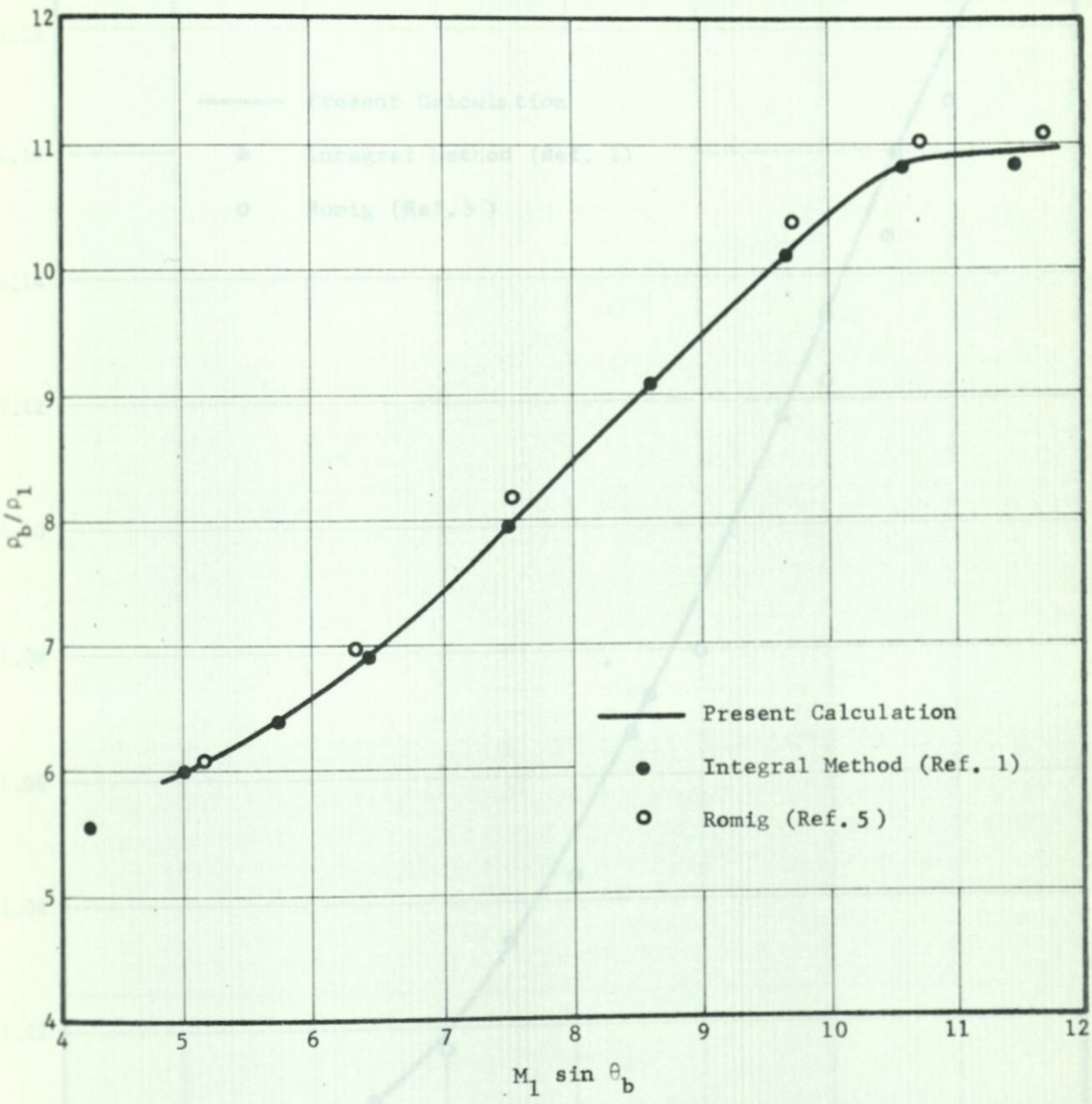

Fig. 6 Variation of Surface Density with Hypersonic Similarity Parameter ($p_1 = 10^{-3}$ atm, $T_1 = 273.16^{\circ}K$) (Equilibrium Flow)

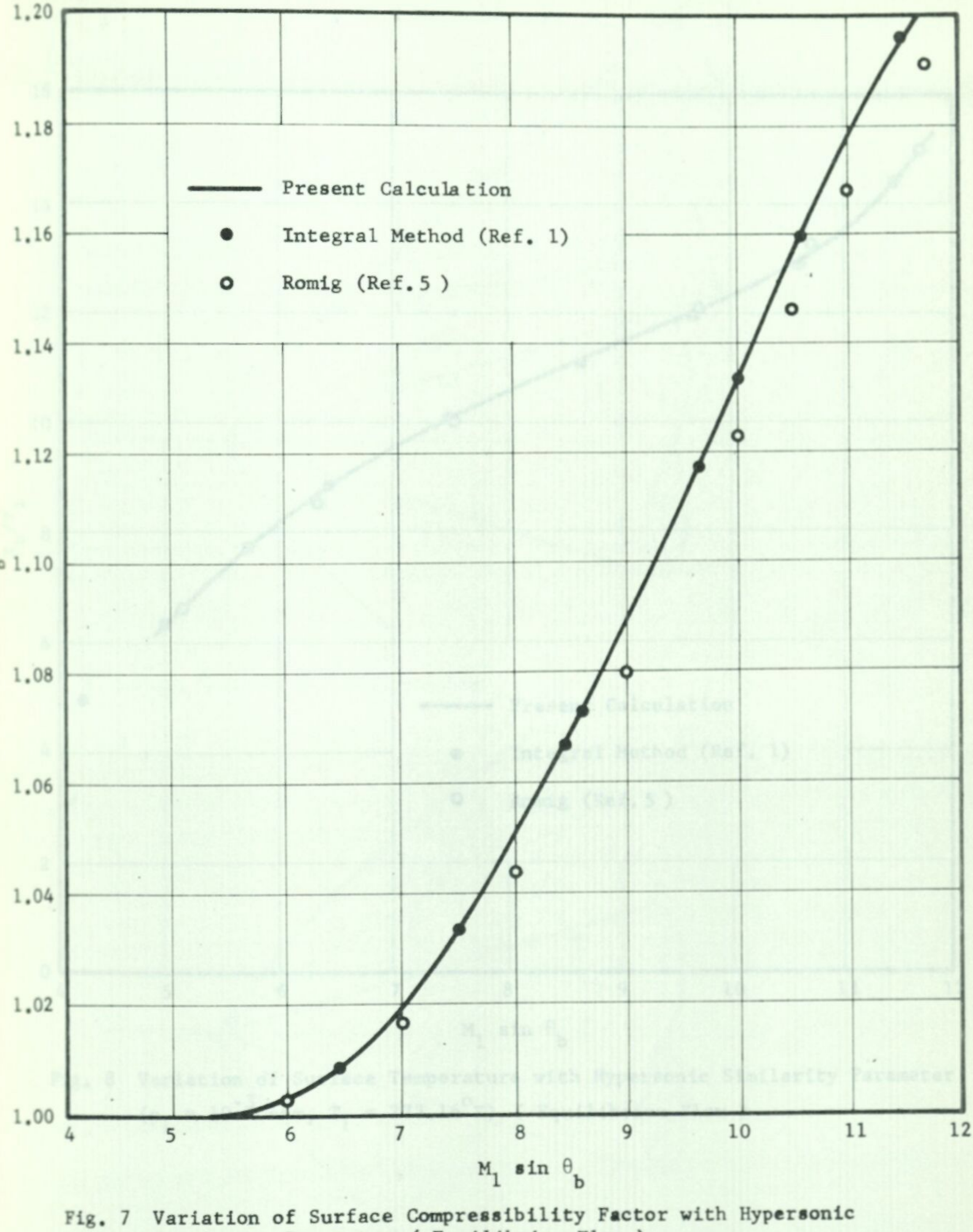

Fig. 7 Variation of Surface Compressibility Factor with Hypersonic Similarity Parameter (Equilibrium Flow)
($p_1 = 10^{-3}$ atm, $T_1 = 273.16^{o}K$)

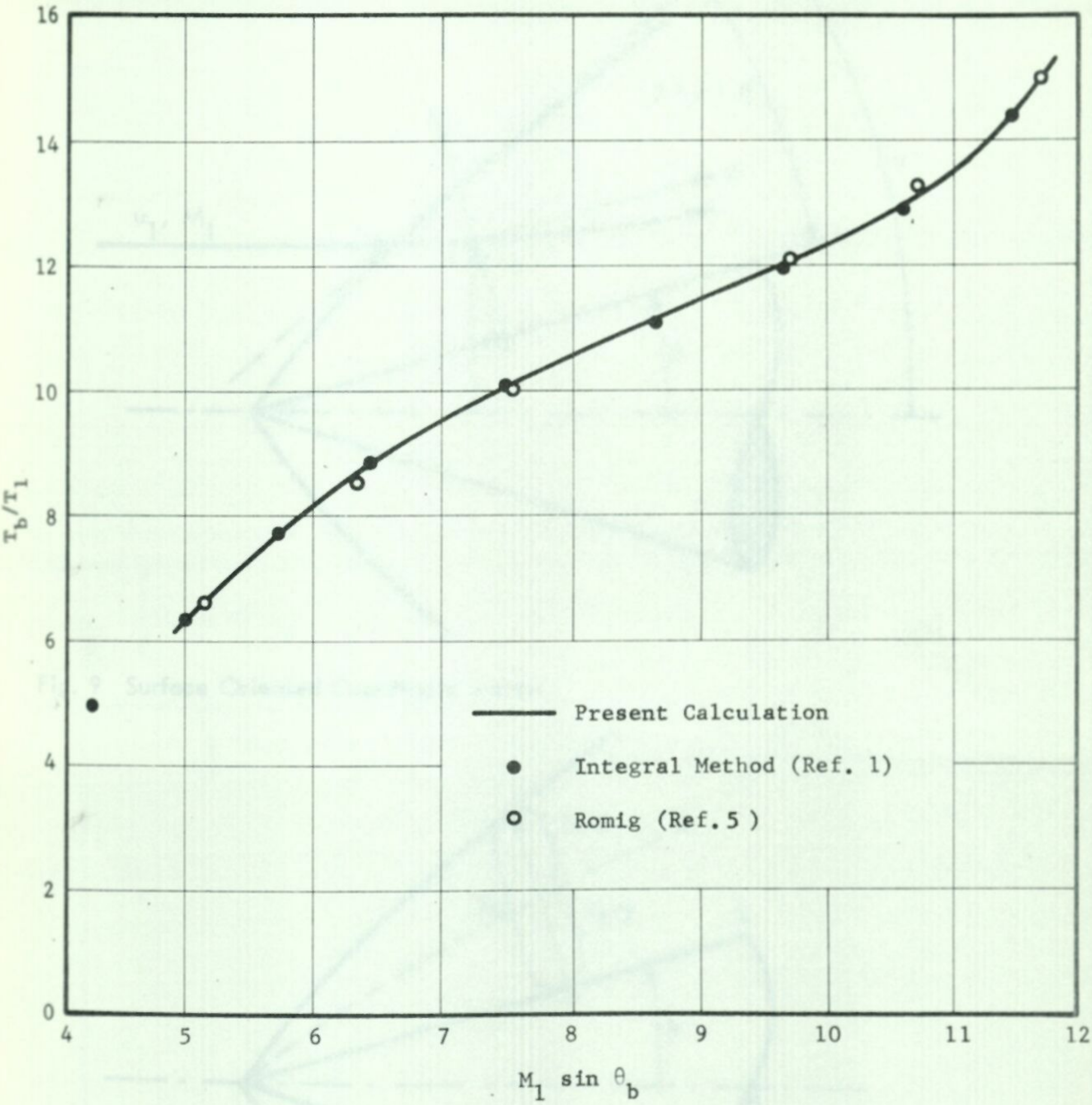

Fig. 8 Variation of Surface Temperature with Hypersonic Similarity Parameter ($p_1 = 10^{-3}$ atm, $T_1 = 273.16^{\circ}K$) (Equilibrium Flow)

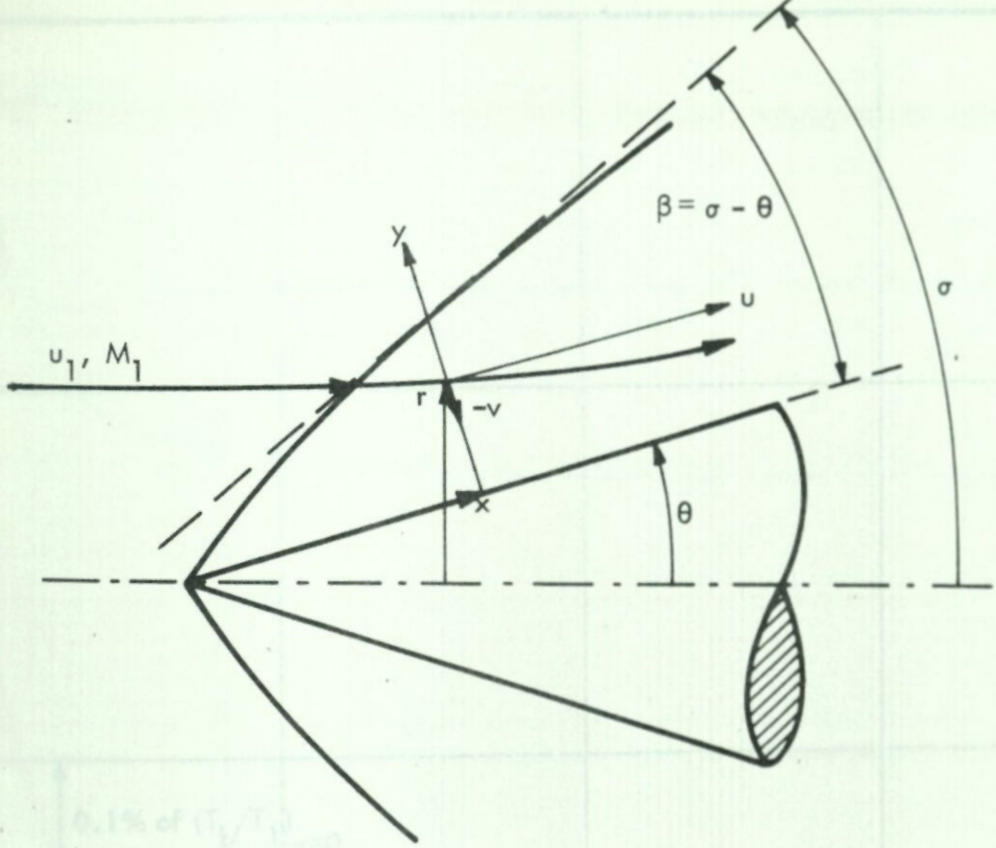

Fig. 9 Surface Oriented Coordinate System

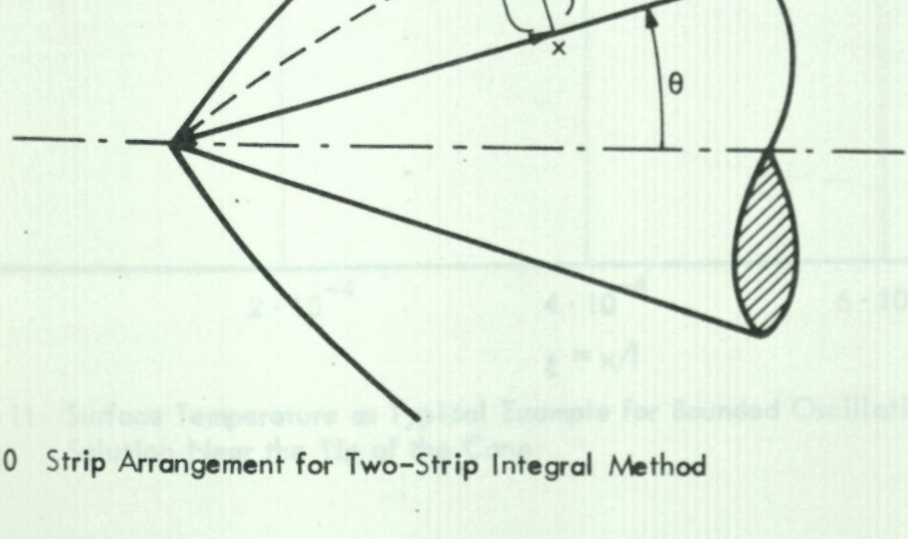

Fig. 10 Strip Arrangement for Two-Strip Integral Method

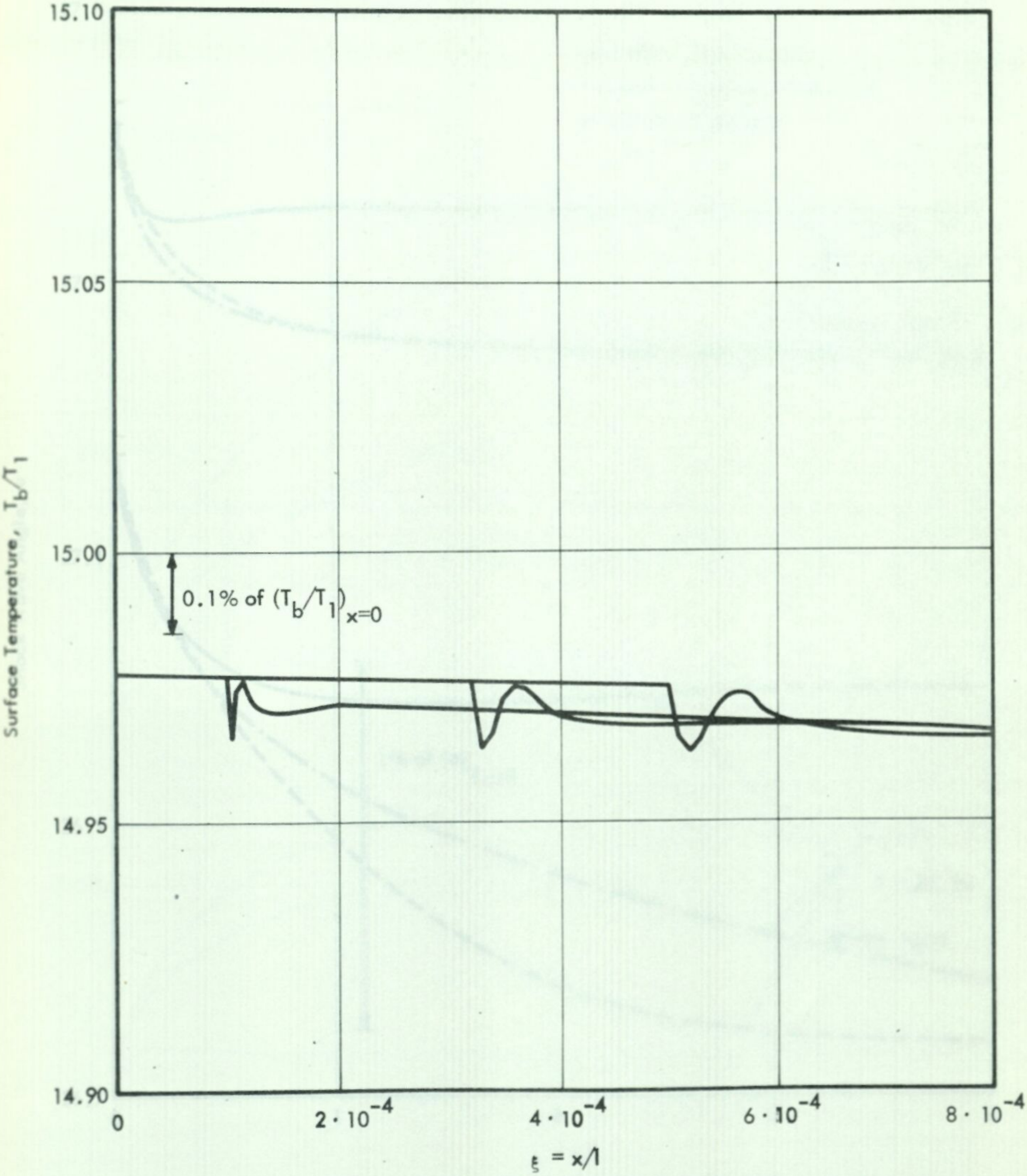

Fig. 11 Surface Temperature as Typical Example for Bounded Oscillations of the Solution Near the Tip of the Cone

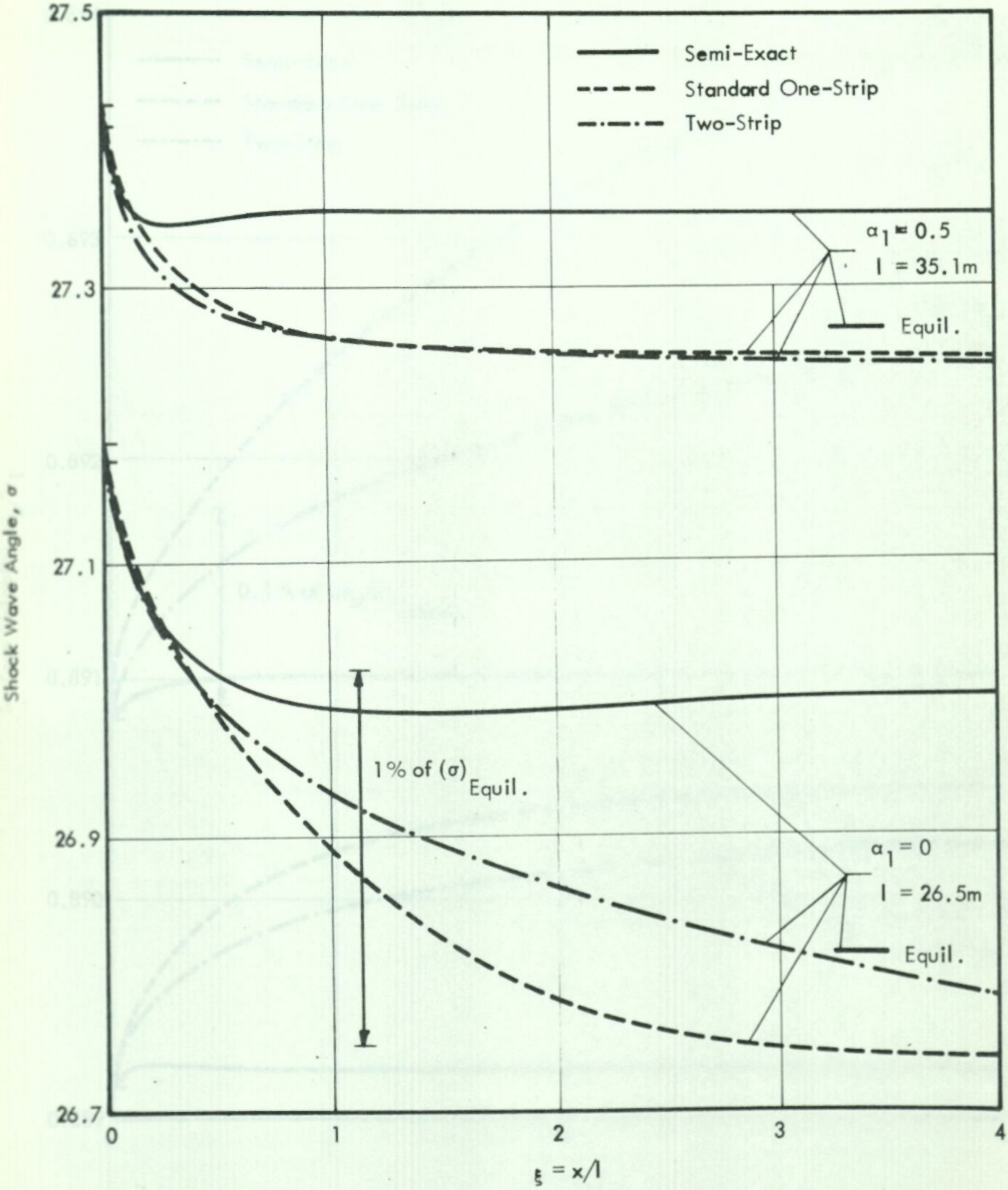

Fig. 12 Shock Wave Angle σ for Nonequilibrium Cone Flow ($\theta = 25^{o}$, $u_1 = 6390$ m/sec, $T_1 = 250^{o}K$, $\rho_1 = 3.9957 \cdot 10^{-3}$ kg/m^3)

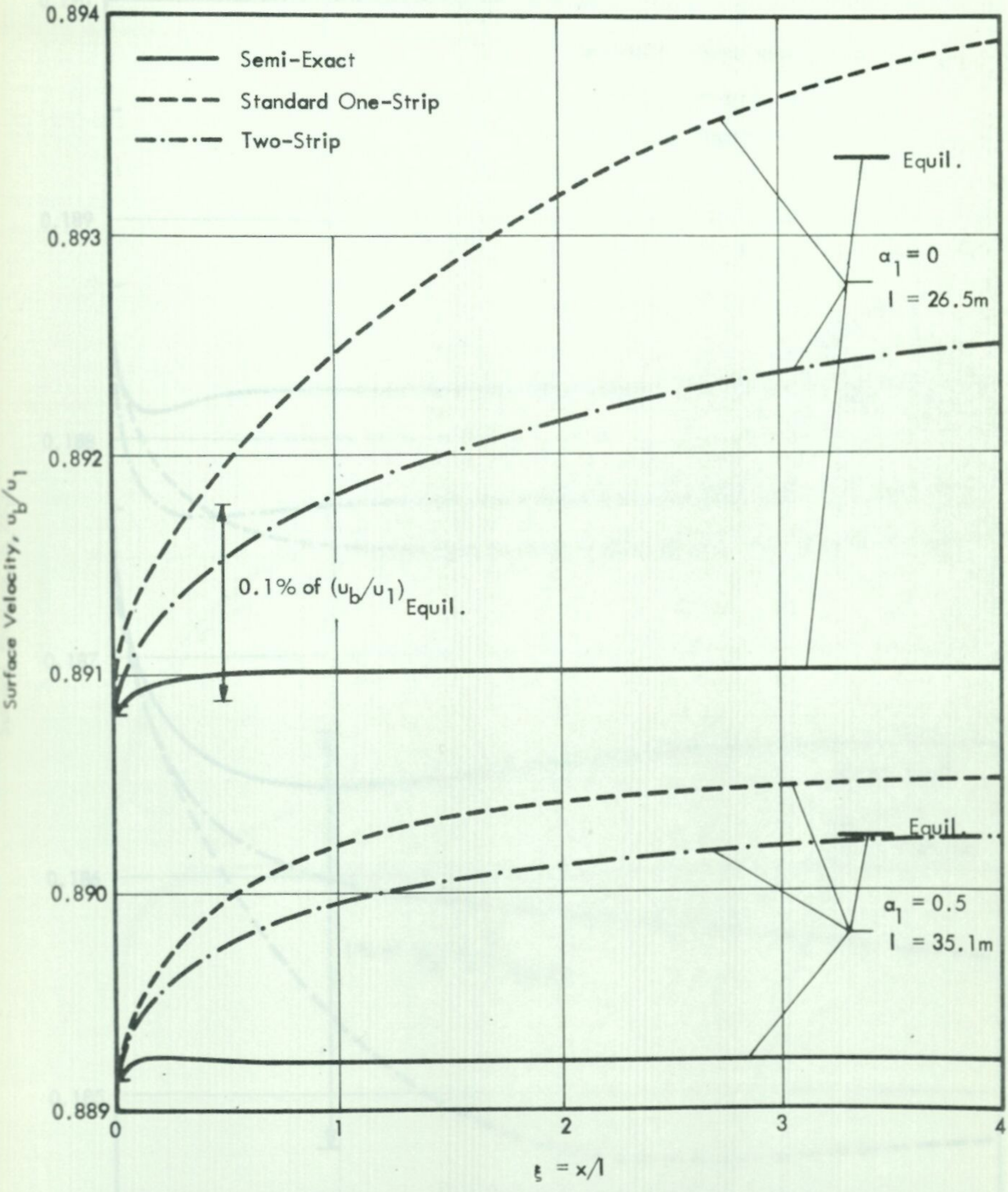

Fig. 13 Surface Velocity u_b for Nonequilibrium Cone Flow ($\theta = 25°$, $u_1 = 6390$ m/sec, $T_1 = 250°K$, $\rho_1 = 3.9957 \cdot 10^{-3}$ kg/m^3)

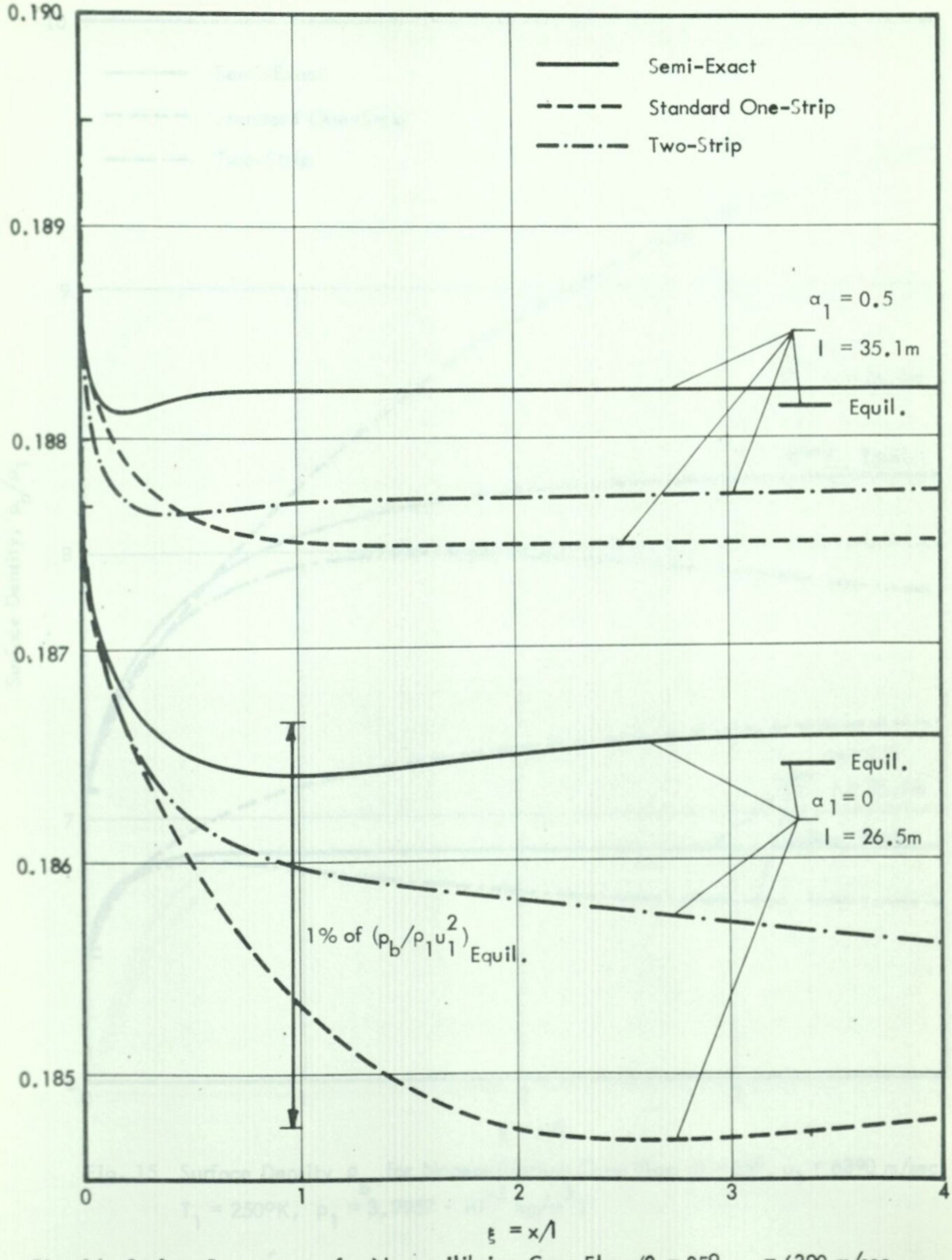

Fig. 14 Surface Pressure p_b for Nonequilibrium Cone Flow ($\theta = 25^o$, $u_1 = 6390$ m/sec, $T_1 = 250^oK$, $\rho_1 = 3.9957 \cdot 10^{-3}$ kg/m^3)

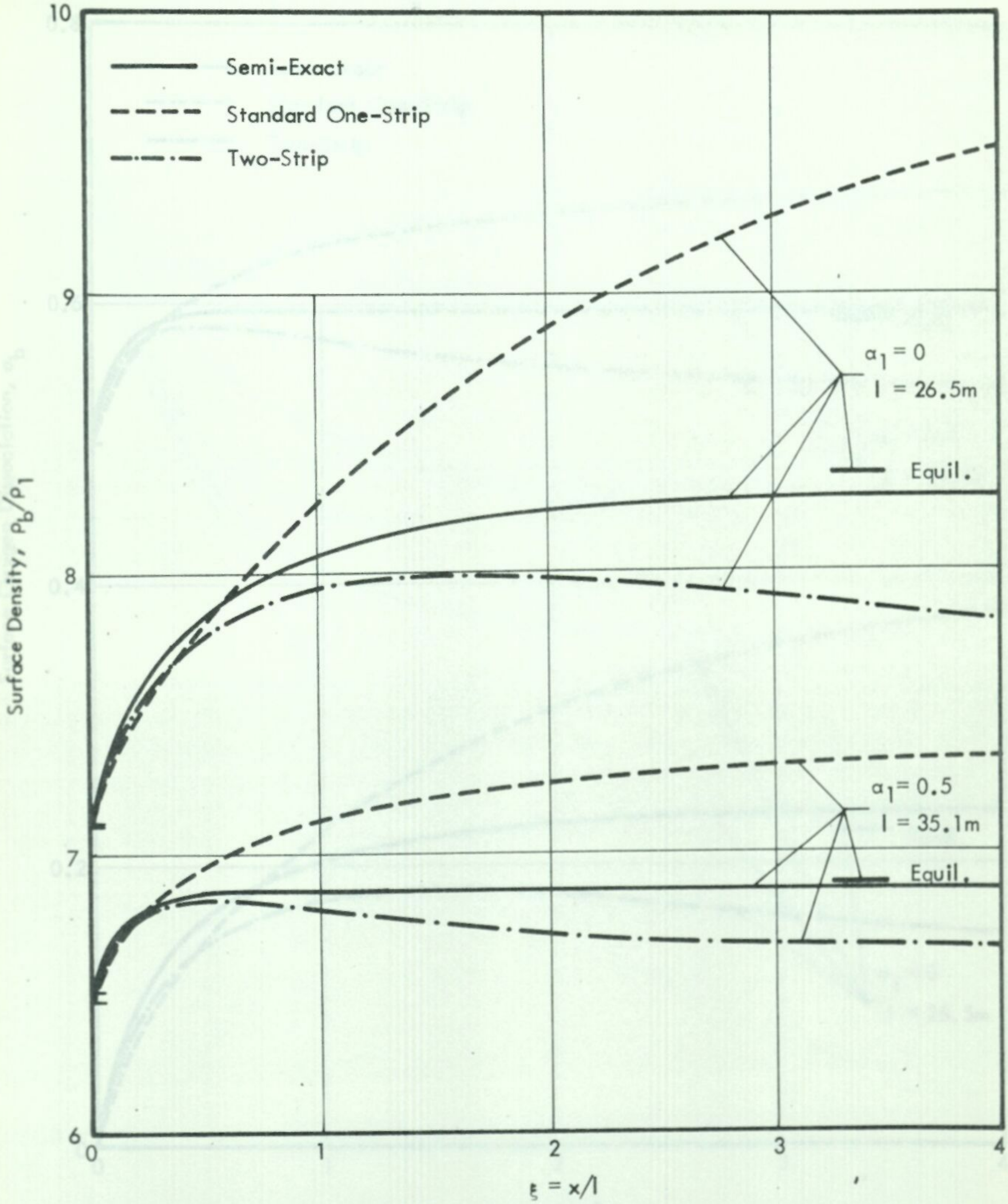

Fig. 15 Surface Density ρ_b for Nonequilibrium Cone Flow ($\theta = 25^o$, $u_1 = 6390$ m/sec, $T_1 = 250^oK$, $\rho_1 = 3.9957 \cdot 10^{-3}$ kg/m^3)

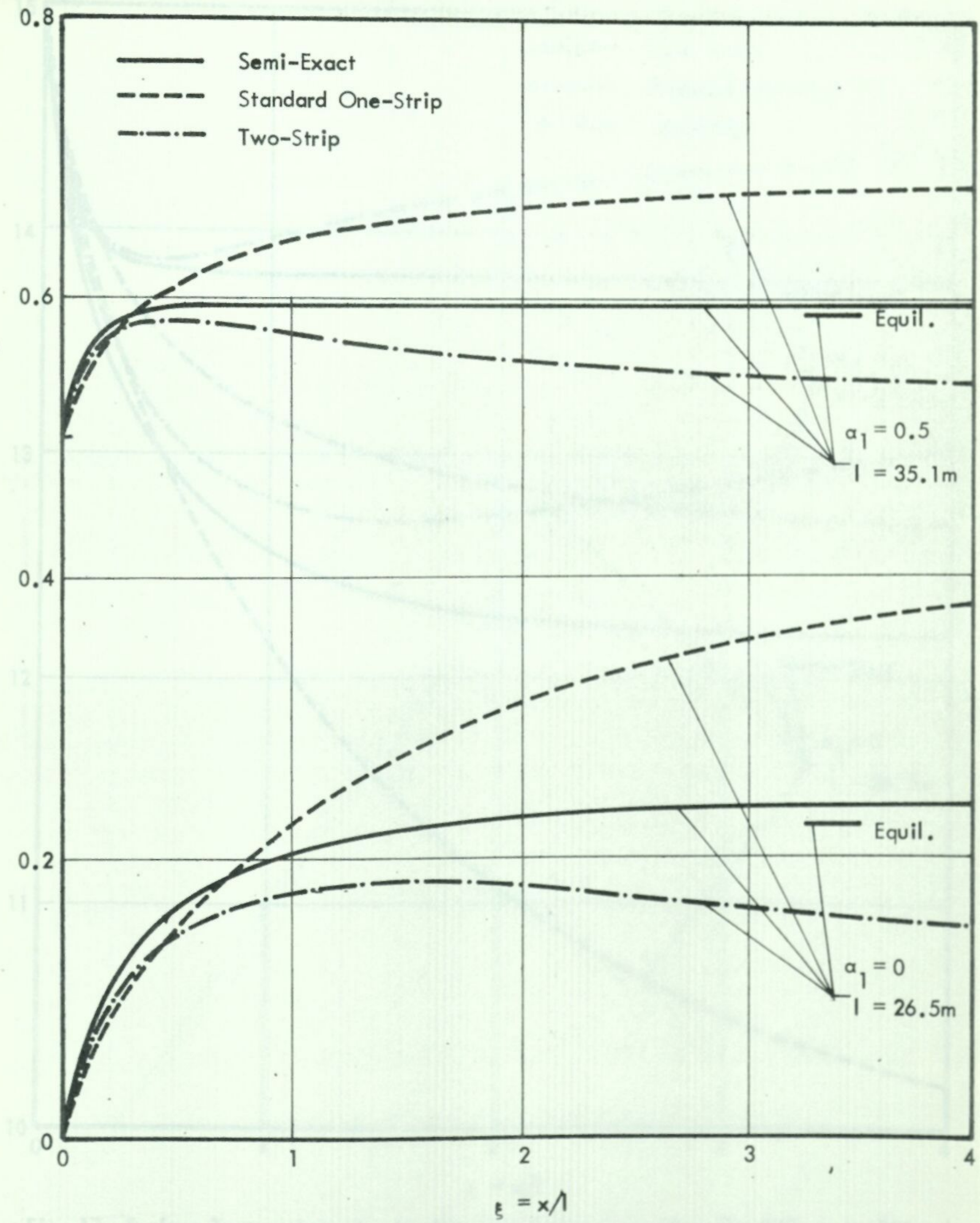

Fig. 16 Surface Dissociation α_b for Nonequilibrium Cone Flow ($\theta = 25^o$, $u_1 = 6390$ m/sec, $T_1 = 250^oK$, $\rho_1 = 3.9957 \cdot 10^{-3}$ kg/m^3)

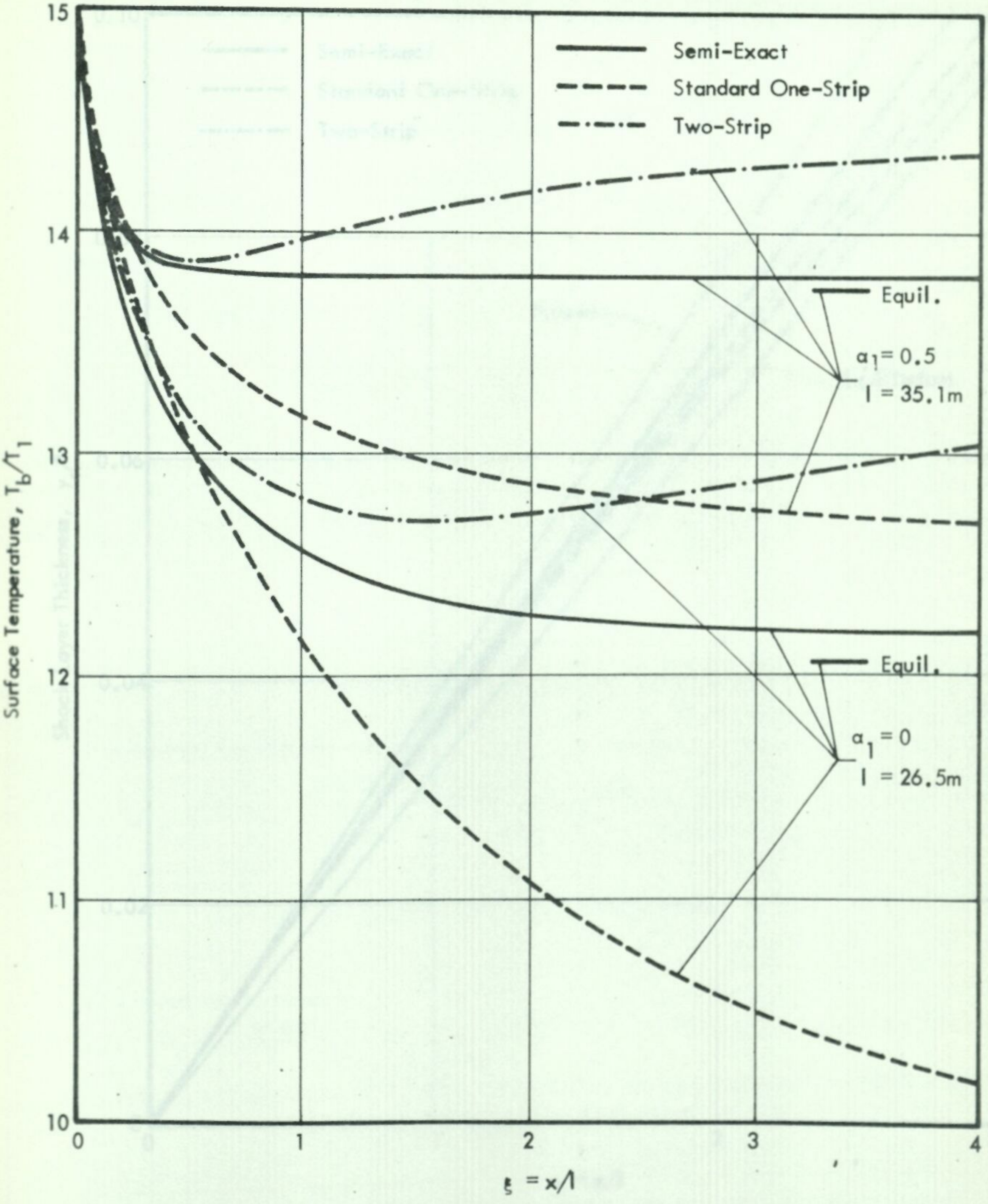

Fig. 17 Surface Temperature T_b for Nonequilibrium Cone Flow ($\theta = 25°$, $u_1 = 6390$ m/sec, $T_1 = 250°K$, $\rho_1 = 3.9957 \cdot 10^{-3}$ kg/m^3)

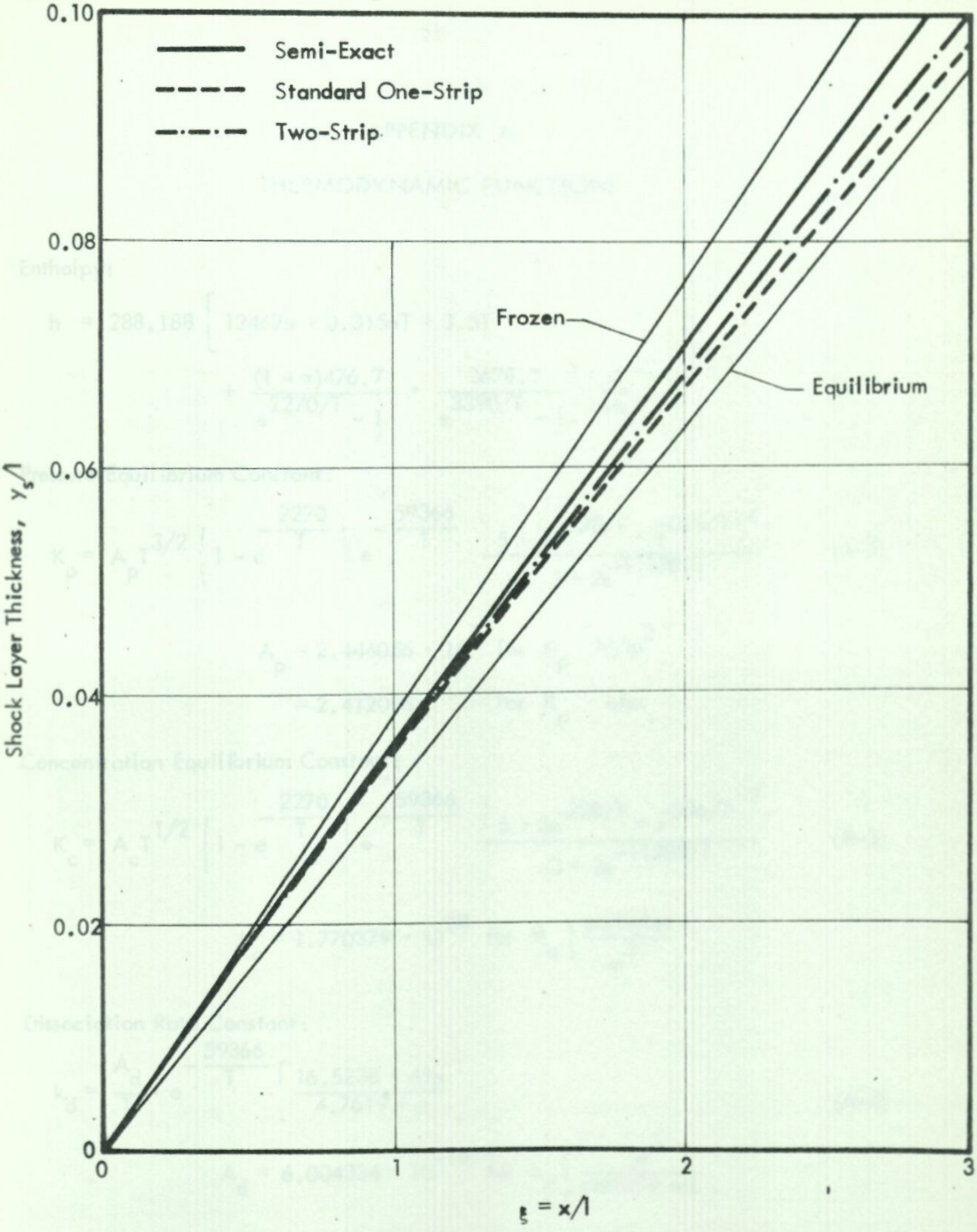

Fig. 18 Shock Layer Thickness y_s for Nonequilibrium Cone Flow ($\theta = 25°$, $u_1 = 6390$ m/sec, $T_1 = 250°K$, $\rho_1 = 3.9957 \cdot 10^{-3}$ kg/m^3)

APPENDIX A

THERMODYNAMIC FUNCTIONS

Enthalpy:

$$h = 288.188 \left[12467\alpha + 0.315\alpha T + 3.5T + \frac{(1-\alpha)476.7}{e^{2270/T} - 1} + \frac{2678.1}{e^{3390/T} - 1} \right] \left[\frac{J}{kg} \right] \tag{A-1}$$

Pressure Equilibrium Constant:

$$K_p = A_p T^{3/2} \left(1 - e^{-\frac{2270}{T}} \right) e^{-\frac{59366}{T}} \frac{\left(5 + 3e^{-228/T} + e^{-326/T} \right)^2}{3 + 2e^{-11390/T}} \tag{A-2}$$

$$A_p = 2.444056 \cdot 10^5 \quad \text{for } K_p \left[N/m^2 \right]$$

$$= 2.412096 \quad \text{for } K_p \left[atm \right]$$

Concentration Equilibrium Constant:

$$K_c = A_c T^{1/2} \left(1 - e^{-\frac{2270}{T}} \right) e^{-\frac{59366}{T}} \frac{\left(5 + 3e^{-228/T} + e^{-326/T} \right)^2}{3 + 2e^{-11390/T}} \tag{A-3}$$

$$A_c = 1.770379 \cdot 10^{28} \quad \text{for } K_c \left[\frac{particles}{m^3} \right]$$

Dissociation Rate Constant:

$$k_d = \frac{A_d}{T} \cdot e^{-\frac{59366}{T}} \left[\frac{16.5238 + 41\alpha}{4.7619 + \alpha} \right] \tag{A-4}$$

$$A_d = 6.004334 \cdot 10^{-12} \quad \text{for } k_d \left[\frac{m^3}{particle\ sec} \right]$$

The above expressions were taken from Ref. 1.

APPENDIX B

SHOCK WAVE RELATIONS FOR FROZEN COMPOSITION ACROSS THE SHOCK

$$T_s = \frac{u_1 \sin\sigma}{RZ_1}\left(1 + \frac{RZ_1 T_1}{u_1^2 \sin^2\sigma}\right)\sqrt{(u_1 \sin\sigma)^2 - 2(h_s - h_1)}$$

$$-\frac{1}{RZ_1}\left[(u_1 \sin\sigma)^2 - 2(h_s - h_1)\right] \quad \text{(B-1)}$$

$$\rho_s = \frac{\rho_1 u_1 \sin\sigma}{\sqrt{(u_1 \sin\sigma)^2 - 2(h_s - h_1)}} \quad \text{(B-2)}$$

$$p_s = p_1 \left(\frac{\rho_s}{\rho_1}\right)\left(\frac{T_s}{T_1}\right) \quad \text{(B-3)}$$

$$u_s = \frac{\rho_1}{\rho_s} u_1 \sin\sigma \sin\beta + u_1 \cos\sigma \cos\beta \quad \text{(B-4)}$$

$$v_s = -\frac{\rho_1}{\rho_s} u_1 \sin\sigma \cos\beta + u_1 \cos\sigma \sin\beta \quad \text{(B-5)}$$

$$\frac{dT_s}{dx} = T_1 C_1 \frac{d\sigma}{dx} \quad \text{(B-6)}$$

$$\frac{d\rho_s}{dx} = \rho_1 C_2 \frac{d\sigma}{dx} \quad \text{(B-7)}$$

$$\frac{dp_s}{dx} = RZ_s(\rho_s T_1 C_1 + \rho_1 T_s C_2)\frac{d\sigma}{dx} \quad \text{(B-8)}$$

$$\frac{du_s}{dx} = u_1 C_3 \frac{d\sigma}{dx} \quad \text{(B-9)}$$

$$\frac{dv_s}{dx} = u_1 C_4 \frac{d\sigma}{dx} \quad \text{(B-10)}$$

where the dimensionless functions C_i are:

$$C_1 = 2u_1 \cos\sigma \left[(u_1 \sin\sigma)^2 - u_1 \sin\sigma \sqrt{(u_1 \sin\sigma)^2 - 2(h_s - h_1)} - (h_s - h_1)\left(1 - \frac{RZ_1T_1}{u_1^2 \sin^2\sigma}\right)\right] \left\{ T_1 \left[(RZ_1 - 2S_s)\sqrt{(u_1 \sin\sigma)^2 - 2(h_s - h_1)} + u_1 \sin\sigma \left(1 + \frac{RZ_1T_1}{u_1^2 \sin^2\sigma}\right) S_s \right] \right\}^{-1} \tag{B-11}$$

$$C_2 = \frac{u_1 \cos\sigma}{\sqrt{(u_1 \sin\sigma)^2 - 2(h_s - h_1)}} + \frac{u_1 \sin\sigma (T_1 S_s C_1 - u_1^2 \sin\sigma \cos\sigma)}{\left[(u_1 \sin\sigma)^2 - 2(h_s - h_1)\right]^{3/2}} \tag{B-12}$$

$$C_3 = \left(\frac{\rho_1}{\rho_s} - 1\right)(\sin\sigma \cos\beta + \cos\sigma \sin\beta) - \left(\frac{\rho_1}{\rho_s}\right)^2 \sin\sigma \sin\beta \, C_2 \tag{B-13}$$

$$C_4 = \left(\frac{\rho_1}{\rho_s} - 1\right)(\sin\sigma \sin\beta - \cos\sigma \cos\beta) + \left(\frac{\rho_1}{\rho_s}\right)^2 \sin\sigma \cos\beta \, C_2 \tag{B-14}$$

APPENDIX C

COEFFICIENTS AND FUNCTIONS IN EQUATIONS (4.39) THROUGH (4.46)

$$a_{11} = u_b^2 \tag{C-1}$$

$$a_{12} = -\rho_b S_b \tag{C-2}$$

$$a_{13} = -\rho_b L_b \tag{C-3}$$

$$a_{18} = -u_b(1 + \delta \cot \theta)(\rho_1 u_s C_2 + \rho_s u_1 C_3) \tag{C-4}$$

$$a_{24} = u_2^2 \tag{C-5}$$

$$a_{25} = -\rho_2 S_2 \tag{C-6}$$

$$a_{26} = -\rho_2 L_2 \tag{C-7}$$

$$a_{27} = \rho_2 v_2 \tag{C-8}$$

$$a_{28} = u_2 C_5(\rho_1 u_s C_2 + \rho_s u_1 C_3) \tag{C-9}$$

$$a_{31} = RZ_b T_b + u_b^2 \tag{C-10}$$

$$a_{32} = \rho_b(RZ_b - 2S_b) \tag{C-11}$$

$$a_{33} = \rho_b(RbT_b - 2L_b) \tag{C-12}$$

$$a_{38} = -(1 + \delta \cot \theta)\left[\rho_s RZ_s T_1 C_1 + \rho_1(RZ_s T_s + u_s^2)C_2 + 2\rho_s u_1 u_s C_3\right] \tag{C-13}$$

$$a_{44} = RZ_2 T_2 + u_2^2 \tag{C-14}$$

$$a_{45} = \rho_2(RZ_2 - 2S_2) \tag{C-15}$$

$$a_{46} = \rho_2(RbT_2 - 2L_2) \tag{C-16}$$

$$a_{47} = -2\rho_2 v_2 \tag{C-17}$$

$$a_{48} = C_5[\rho_s RZ_s T_1 C_1 + \rho_1(RZ_s T_s + u_s^2)C_2 + 2\rho_s u_1 u_s C_3)] \tag{C-18}$$

$$a_{58} = (1 + \delta \cot\theta)(\rho_1 u_s v_s C_2 + \rho_s u_1 v_s C_3 + \rho_s u_1 u_s C_4) \tag{C-19}$$

$$a_{64} = u_2^2 v_2 \tag{C-20}$$

$$a_{65} = -\rho_2 v_2 S_2 \tag{C-21}$$

$$a_{66} = -\rho_2 v_2 L_2 \tag{C-22}$$

$$a_{67} = \rho_2(u_2^2 - v_2^2) \tag{C-23}$$

$$a_{68} = u_2 C_5(\rho_1 u_s v_s C_2 + \rho_s u_1 v_s C_3 + \rho_s u_1 u_s C_4) \tag{C-24}$$

$$a_{71} = a_{11}\alpha_b \tag{C-25}$$

$$a_{72} = a_{12}\alpha_b \tag{C-26}$$

$$a_{73} = a_{13}\alpha_b + \rho_b u_b^2 \tag{C-27}$$

$$a_{78} = a_{18}\alpha_s \tag{C-28}$$

$$a_{84} = a_{24}\alpha_2 \tag{C-29}$$

$$a_{85} = a_{25}\alpha_2 \tag{C-30}$$

$$a_{86} = a_{26}\alpha_2 + \rho_2 u_2^2 \tag{C-31}$$

$$a_{87} = a_{27}\alpha_2 \tag{C-32}$$

$$a_{88} = a_{28}\alpha_s \tag{C-33}$$

$$A_1 = \frac{u_b}{x}\left[\frac{1}{\delta}\left([2\rho_2 u_2(2+\delta\cot\theta) - 3\rho_s u_s(1+\delta\cot\theta) - \rho_b u_b]\tan\beta + 4[\rho_s v_s(1+\delta\cot\theta) - \rho_2 v_2(2+\delta\cot\theta)]\right) - \rho_b u_b + \rho_s u_s(1+\cot\theta\tan\beta)\right] \tag{C-34}$$

$$A_2 = \frac{u_2}{x}\left[\frac{1}{\delta}\left([2\rho_s u_s C_5 - \rho_2 u_2]\,2\tan\beta + 2\rho_2 v_2 - 5\rho_s v_s C_5\right) - \rho_s u_s C_6 - \rho_2 u_2 C_7\right] \tag{C-35}$$

$$A_3 = \frac{1}{x}\left[\frac{1}{\delta}\left([2(p_2 + \rho_2 u_2^2)(2+\delta\cot\theta) - 3(p_s + \rho_s u_s^2)(1+\delta\cot\theta) - (p_b + \rho_b u_b^2)]\tan\beta + 4[\rho_s u_s v_s(1+\delta\cot\theta) - \rho_2 u_2 v_2(2+\delta\cot\theta\right) - p_s - \rho_b u_b^2 + (p_s + \rho_s u_s^2)(1+\cot\theta\tan\beta)\right] \tag{C-36}$$

$$A_4 = \frac{1}{x}\left[\frac{1}{\delta}\left([2(p_s + \rho_s u_s^2)C_5 - (p_2 + \rho_2 u_2^2)]\,2\tan\beta + 2\rho_2 u_2 v_2 - 5\rho_s u_s v_s C_5\right) \frac{2p_2 + p_s}{2+\delta\cot\theta} - (p_s + \rho_s u_s^2)C_6 - (p_2 + \rho_2 u_2^2)C_7\right] \tag{C-37}$$

$$A_5 = \frac{1}{x}\left[\frac{1}{\delta}\left([3\rho_s u_s v_s(1+\delta\cot\theta) - 2\rho_2 u_2 v_2(2+\delta\cot\theta)]\tan\beta - 4[p_b + (p_s + \rho_s v_s^2)(1+\delta\cot\theta) - (p_2 + \rho_2 v_2^2)(2+\delta\cot\theta)]\right) + (p_s - p_b)\cot\theta - \rho_s u_s v_s(1+\cot\theta\tan\beta)\right] \tag{C-38}$$

$$A_6 = \frac{u_2}{x}\left[\frac{1}{\delta}\left([2\rho_s u_s v_s C_5 - \rho_2 u_2 v_2]\,2\tan\beta + \frac{p_b}{2+\delta\cot\theta} - 5(p_s + \rho_s v_s^2)C_5 + 2(p_2 + \rho_2 v_2^2)\right) + \frac{(2p_2 + p_s)\cot\theta}{2+\delta\cot\theta} - \rho_s u_s v_s C_6 - \rho_2 u_2 v_2 C_7\right] \tag{C-39}$$

$$A_7 = \frac{u_b}{x}\left[\frac{1}{\delta}\left([2\rho_2 u_2 \alpha_2 (2 + \delta \cot\theta) - 3\rho_s u_s \alpha_s (1 + \delta \cot\theta) - \rho_b u_b \alpha_b] \tan\beta \right.\right.$$

$$\left. + 4[\rho_s v_s \alpha_s (1 + \delta \cot\theta) - \rho_2 v_2 \alpha_2 (2 + \delta \cot\theta)]\right) - \rho_b u_b \alpha_b$$

$$\left. + \rho_s u_s \alpha_s (1 + \cot\theta \tan\beta)\right] + u_b [\rho_b f_b - \rho_s f_s (1 + \delta \cot\theta)] \qquad \text{(C-40)}$$

$$A_8 = \frac{u_2}{x}\left[\frac{1}{\delta}\left([2\rho_s u_s \alpha_s C_5 - \rho_2 u_2 \alpha_2] 2 \tan\beta + 2\rho_2 v_2 \alpha_2 - 5\rho_s v_s \alpha_s C_5\right) - \rho_s u_s \alpha_s C_6\right.$$

$$\left. - \rho_2 u_2 \alpha_2 C_7\right] + u_2 [\rho_2 f_2 + \rho_s f_s C_5] \qquad \text{(C-41)}$$

C_i $(i = 1, 2, 3, 4)$ are given in Appendix B.

$$C_5 = \frac{1 + \delta \cot\theta}{2 + \delta \cot\theta} \qquad \text{(C-42)}$$

$$C_6 = \frac{1 + \cot\theta \tan\beta}{2 + \delta \cot\theta} \qquad \text{(C-43)}$$

$$C_7 = \frac{2 + \cot\theta \tan\beta}{2 + \delta \cot\theta} \qquad \text{(C-44)}$$

APPENDIX D

COEFFICIENTS AND FUNCTIONS IN EQUATIONS (4.74) THROUGH (4.81)

$$b_{11} = 3u_b \tag{D-1}$$

$$b_{12} = -\frac{3\rho_b S_b}{u_b} \tag{D-2}$$

$$b_{13} = -\frac{3\rho_b L_b}{u_b} \tag{D-3}$$

$$b_{14} = 2(a+1)(2v_2 \cot\beta - u_2) \tag{D-4}$$

$$b_{15} = 2(a+1)\,\frac{\rho_2 S_2}{u_2} \tag{D-5}$$

$$b_{16} = 2(a+1)\,\frac{\rho_2 L_2}{u_2} \tag{D-6}$$

$$b_{17} = 2(a+1)\,\frac{\rho_2}{u_2}\,(v_2 + 2u_2 \cot\beta) \tag{D-7}$$

$$\begin{aligned} b_{18} = {} & a\,[\,\rho_1(u_s - 4v_s \cot\beta)C_2 + \rho_s u_1 C_3 - 4\rho_s u_1 \cot\beta\, C_4\,] \\ & - \frac{1}{\sin 2\beta}\Big[\,2\rho_2 u_2(3a+1) - \rho_s u_s(7a-1) - 2\rho_b u_b + 4\cot\theta\,(\rho_s v_s \\ & - \rho_2 v_2)\Big] + \frac{1}{2\sin^2\beta}\Big[\,[2\rho_2 u_2(a+1) - 3a\rho_s u_s - \rho_b u_b\,]\tan\beta \\ & 4a\rho_s v_s - 4(a+1)\rho_2 v_2\,\Big] \end{aligned} \tag{D-8}$$

$$b_{24} = 2(2u_2 - v_2 \cot\beta) \tag{D-9}$$

$$b_{25} = -4\,\frac{\rho_2 S_2}{u_2} \tag{D-10}$$

$$b_{26} = -4 \; \frac{\rho_2 L_2}{u_2} \tag{D-11}$$

$$b_{27} = -2 \; \frac{\rho_2}{u^2} \; (2v_2 + u_2 \cot \beta) \tag{D-12}$$

$$\begin{aligned} b_{28} = & -\frac{a}{a+1} \left[\rho_1 (2u_s - 5v_s \cot \beta) C_2 + 2\rho_s u_1 C_3 - 5\rho_s u_1 \cot \beta \, C_4 \right] \\ & - \frac{1}{\sin 2\beta \, (a+1)} \left[2(5a-1)\rho_s u_s - 8a\rho_2 u_2 - \cot \theta \, (5\rho_s v_s - 2\rho_2 v_2) \right] \\ & + \frac{1}{2 \sin^2 \beta} \left[\frac{a}{a+1} \; (4\rho_s u_s \tan \beta - 5\rho_s v_s) - \rho_2 (2u_2 \tan \beta - 2v_2) \right] \end{aligned} \tag{D-13}$$

$$b_{31} = 2RT_b Z_1 + 3u_b^2 \tag{D-14}$$

$$b_{32} = 2\rho_b (RZ_1 - 3S_b) \tag{D-15}$$

$$b_{33} = 2\rho_b (bRT_b - 3L_b) \tag{D-16}$$

$$b_{34} = 2(a+1) \left[u_2 (2v_2 \cot \beta - u_2) - RT_2 Z_1 \right] \tag{D-17}$$

$$b_{35} = 2(a+1)\rho_2 \left[\frac{2S_2}{u_2} \; (u_2 - v_2 \cot \beta) - RZ_1 \right] \tag{D-18}$$

$$b_{36} = 2(a+1)\rho_2 \left[\frac{2L_2}{u_2} \; (u_2 - v_2 \cot \beta) - bRT_2 \right] \tag{D-19}$$

$$b_{37} = 4(a+1)\rho_2 \left[\frac{v_2}{u_2} \; (u_2 - v_2 \cot \beta) + u_2 \cot \beta \right] \tag{D-20}$$

$$\begin{aligned} b_{38} = & (a+1) RZ_1 \rho_s T_1 C_1 + \left[(a+1) \, RZ_1 T_s + a u_s (u_s - 4v_s \cot \beta) \right] \rho_1 C_2 + 2a\rho_s (u_s \\ & - 4v_s \cot \beta) u_1 C_3 - 4a\rho_s u_1 u_s \cot \beta \, C_4 - \frac{1}{\sin 2\beta} \Big[\, 2(p_2 + \rho_2 u_2^2)(3a+1) \\ & - (p_s + \rho_s u_s^2)(7a-1) - 2(p_b + \rho_b u_b^2) + 4 \cot \theta \, (\rho_s u_s v_s - \rho_2 u_2 v_2) \Big] \\ & + \frac{1}{2 \sin^2 \beta} \Big[\left[2(p_2 + \rho_2 u_2^2)(a+1) - 3a(p_s + \rho_s u_s^2) - (p_b + \rho_b u_b^2) \right] \tan \beta \\ & + 4 \left[\rho_s u_s v_s a - \rho_2 u_2 v_2 (a+1) \right] \Big] \end{aligned} \tag{D-21}$$

$$b_{44} = 2\left[u_2(2u_2 - v_2 \cot\beta) + \frac{2a+1}{a+1} RT_2 Z_1 \right] \tag{D-22}$$

$$b_{45} = 2\rho_2 \left[\frac{S_2}{u_2} (v_2 \cot\beta - 4u_2) + \frac{2a+1}{a+1} RZ_1 \right] \tag{D-23}$$

$$b_{46} = 2\rho_2 \left[\frac{L_2}{u_2} (v_2 \cot\beta - 4u_2) + \frac{2a+1}{a+1} bRT_2 \right] \tag{D-24}$$

$$b_{47} = 2\rho_2 \left[\frac{v_2}{u_2} (v_2 \cot\beta - 4u_2) - u_2 \cot\beta \right] \tag{D-25}$$

$$\begin{aligned} b_{48} = {} & -\frac{1}{a+1} \Big[(2a+1)RZ_1\rho_s T_1 C_1 + \big[(2a+1)RZ_1 T_s + u_s a(2u_s - 5v_s \cot\beta)\big]\rho_1 C_2 \\ & + \rho_s a(4u_s - 5v_s \cot\beta)u_1 C_3 - 5a\rho_s u_1 u_s \cot\beta \; C_4 \Big] - \frac{1}{(a+1)\sin 2\beta} \Big[2(p_s \\ & \quad + \rho_s u_s^2)(5a-1) - 8a(p_2 + \rho_2 u_2^2) + \cot\theta(2\rho_2 u_2 v_2 - 5\rho_s u_s v_s) \Big] \\ & \quad + \frac{1}{2\sin^2\beta} \Big[\Big[\frac{4a}{a+1} (p_s + \rho_s u_s^2) - 2(p_2 + \rho_2 u_2^2) \Big] \tan\beta \\ & \qquad + 2\rho_2 u_2 v_2 - \frac{5a}{a+1} \rho_s u_s v_s \Big] \end{aligned} \tag{D-26}$$

$$b_{51} = (a+3)RT_b Z_1 \cot\beta \tag{D-27}$$

$$b_{52} = (a+3)R\rho_b Z_1 \cot\beta \tag{D-28}$$

$$b_{53} = (a+3)RbT_b\rho_b \cot\beta \tag{D-29}$$

$$b_{54} = 2(a+1)\left[v_2(u_2 - 2v_2 \cot\beta) - 2RT_2 Z_1 \cot\beta \right] \tag{D-30}$$

$$b_{55} = -2(a+1)\rho_2 \left[\frac{v_2 S_2}{u_2} + 2RZ_1 \cot\beta \right] \tag{D-31}$$

$$b_{56} = -2(a+1)\rho_2 \left[\frac{v_2 L_2}{u_2} + 2RbT_2 \cot\beta \right] \tag{D-32}$$

$$b_{57} = -2(a+1)\rho_2 \left[\frac{v_2^2}{u_2} - (u_2 - 4v_2 \cot\beta) \right] \tag{D-33}$$

$$
\begin{aligned}
b_{58} = {} & (4a \cot\beta - \cot\theta) R Z_1 \rho_s T_1 C_1 + \left[a v_s (4 v_s \cot\beta - u_s) + (4a \cot\beta \right. \\
& \left. - \cot\theta) R Z_1 T_s \right] \rho_1 C_2 - a \rho_s u_1 v_s C_3 + a \rho_s (8 v_s \cot\beta - u_s) u_1 C_4 \\
& - \frac{1}{\sin 2\beta} \Big[(7a - 1) \rho_s u_s v_s - 2(3a + 1) \rho_2 u_2 v_2 + 4 \cot\theta \left[(p_2 \right. \\
& \left. + \rho_2 v_2^2) - (p_s + \rho_s v_s^2) \right] \Big] + \frac{1}{2 \sin^2\beta} \Big[\left[3a \rho_s u_s v_s \right. \\
& \left. - 2(a + 1) \rho_2 u_2 v_2 \right] \tan\beta - 4 \left[p_b + (p_s + \rho_s v_s^2)\, a \right. \\
& \left. - (p_2 + \rho_2 v_2^2)(a + 1) \right] \Big] \qquad \text{(D-34)}
\end{aligned}
$$

$$b_{61} = \frac{b_{51}}{a + 3} \qquad \text{(D-35)}$$

$$b_{62} = \frac{b_{52}}{a + 3} \qquad \text{(D-36)}$$

$$b_{63} = \frac{b_{53}}{a + 3} \qquad \text{(D-37)}$$

$$b_{64} = 2 \left[(a + 1) v_2 (v_2 \cot\beta - 2u_2) + 2aRT_2 Z_1 \cot\beta \right] \qquad \text{(D-38)}$$

$$b_{65} = 4\rho_2 \left[(a + 1) \frac{v_2}{u_2} S_2 + aRZ_1 \cot\beta \right] \qquad \text{(D-39)}$$

$$b_{66} = 4\rho_2 \left[(a + 1) \frac{v_2}{u_2} L_2 + abRT_2 \cot\beta \right] \qquad \text{(D-40)}$$

$$b_{67} = 4\rho_2 (a + 1) \left[\frac{v_2^2}{u_2} - (u_2 - v_2 \cot\beta) \right] \qquad \text{(D-41)}$$

$$
\begin{aligned}
b_{68} = {} & - (4a + 1) \rho_s T_1 R Z_1 \cot\beta\, C_1 + \rho_1 \left[a v_s (2u_s - 5 v_s \cot\beta) - (4a + 1) R Z_1 T_s \cot\beta \right] C_2 \\
& + 2a \rho_s u_1 v_s C_3 + 2a \rho_s (u_s - 5 v_s \cot\beta) u_1 C_4 - \frac{1}{\sin 2\beta} \left[8a \rho_2 u_2 v_2 \right. \\
& \left. - 2 \cot\theta (p_2 + \rho_2 v_2^2) + 5 \cot\theta (p_s + \rho_s v_s^2) - 2(5a - 1) \rho_s u_s v_s \right] \\
& + \frac{1}{2 \sin^2\beta} \Big[\left[\rho_2 u_2 v_2 (a + 1) - 2a \rho_s u_s v_s \right] 2 \tan\beta \\
& - p_b + 5a (p_s + \rho_s v_s^2) - 2(a + 1)(p_2 + \rho_2 v_2^2) \Big] \qquad \text{(D-42)}
\end{aligned}
$$

$$b_{71} = b_{11}\alpha_1 \tag{D-43}$$

$$b_{72} = b_{12}\alpha_1 \tag{D-44}$$

$$b_{73} = b_{13}\alpha_1 + 3\rho_b u_b \tag{D-45}$$

$$b_{74} = b_{14}\alpha_1 \tag{D-46}$$

$$b_{75} = b_{15}\alpha_1 \tag{D-47}$$

$$b_{76} = 2(a+1)\rho_2 \left[\frac{L_2\alpha_1}{u_2} + (2v_2 \cot\beta - u_2) \right] \tag{D-48}$$

$$b_{77} = b_{17}\alpha_1 \tag{D-49}$$

$$b_{78} = b_{18}\alpha_1 \tag{D-50}$$

$$b_{84} = b_{24}\alpha_1 \tag{D-51}$$

$$b_{85} = b_{25}\alpha_1 \tag{D-52}$$

$$b_{86} = 2\rho_2 \left[(2u_2 - v_2 \cot\beta) - 2\,\frac{L_2\alpha_1}{u_2} \right] \tag{D-53}$$

$$b_{87} = b_{27}\alpha_1 \tag{D-54}$$

$$b_{88} = b_{28}\alpha_1 \tag{D-55}$$

$$B_7 = \rho_b f_b - \rho_s f_s a \tag{D-56}$$

$$B_8 = \rho_2 f_2 + \frac{a}{a+1}\,\rho_s f_s \tag{D-57}$$

where

$$a = 1 + \cot\theta \tan\beta \tag{D-58}$$

3/17/66
ct

UAR 2 distribution

1	copy	Barbara Davis
1	"	Mrs Williams
"	"	Mr. Croker
"	"	Gorgas Library
1	"	Dr. Herman
"	"	Dr. Arendale
~~"~~	~~"~~	~~Mr. Roy Bland~~
"	"	John McClurkin
"	"	John McDaniel
1	"	UAR 2 report file